Professor **TACHIKAWA Yasuto**
Department of Civil and Earth Resources Engineering
Graduate School of Engineering, Kyoto University

京都大学
KYOTO UNIVERSITY

Frontiers of Flood Hazard Prediction

Toward Enhancing Flood Disaster Resilience

Sponsored by

TOKIO MARINE GROUP

Date of Issue
March 2026

Abstract

This paper focuses on floods as a water-related disaster, introducing flood hazard prediction methods and examples of flood risk estimation using the prediction information.

First, the concept of predicting water hazards and risks is outlined, and then the fundamental flood prediction methods and their developmental history that underpin flood hazard and risk estimation are described.

Next, an analysis of changes in the frequency and intensity of extreme floods due to global warming is analyzed for major rivers in Japan and Southeast Asia as examples.

Then, research on improving the accuracy of rainfall-runoff simulation models, a fundamental technique for enhancing the prediction accuracy of water disaster hazards and risks is discussed.

Finally, it summarizes future technical challenges for improving water disaster resilience.

Contents

Executive Summary

In order to assess flood risk, it is necessary to predict floods with return periods exceeding one hundred years. If we have several hundred years of flow rate time series data, we can statistically analyze it to predict the magnitude of rare floods with return periods of two hundred years or more.

Although such long-term flow observation data does not exist, recently ensemble climate information databases corresponding to observation periods of several thousand years have been created using climate prediction models.

Using the precipitation data in the database, it is now possible to predict flood information corresponding to a return period of several hundred years.

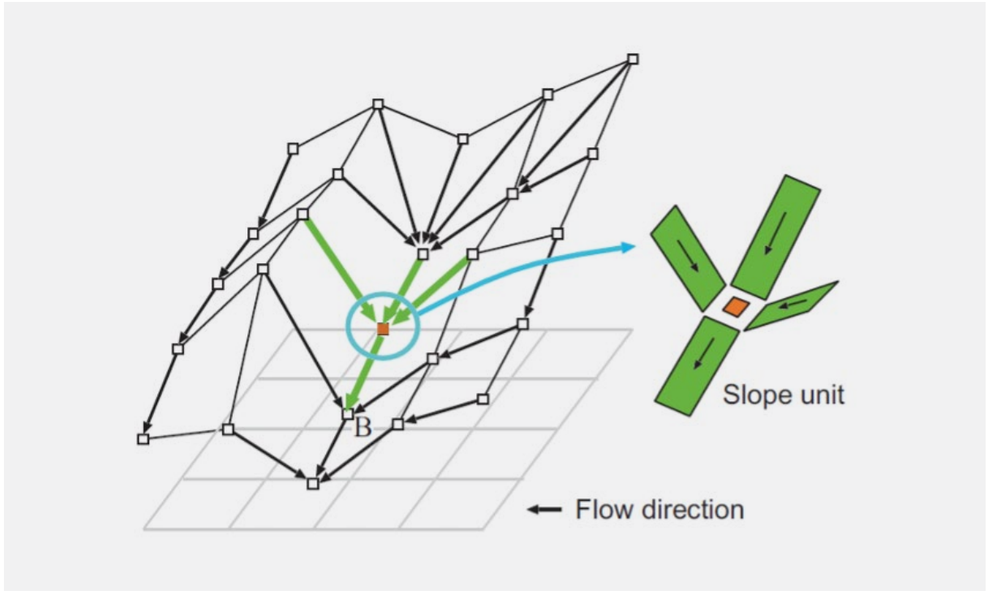

Figure 1: *Watershed topography representation using digital elevation data and its use in distributed rainfall-runoff modeling.*

This report introduces an example of study that predicted changes in flood frequency distributions due to global warming using the distributed rainfall-runoff simulation model 1K-DHM. This model incorporates spatial distribution information such as topography, land cover, surface soil, and geology as shown in Figure 1. The global warming scenario information used was the “Database for Policy Decision making for Future climate change (d4PDF)”, an ensemble climate prediction database contributing to global warming countermeasures.

Figure 2 shows the frequency distribution of annual maximum hourly discharge simulated for the Hirakata site in the Yodo River basin. In the warming scenario with an increase of 4 degrees Celsius, the annual maximum flow discharge is larger than the past experiment with the current climate scenario for all sea surface temperature distribution patterns. The increase rate was greater for higher non-exceedance probabilities (longer return periods).

Comparing the 200-year return period annual maximum flow between the past experiment and the 4-degree increase warming experiment, the increase was 1.5 to 1.7-fold. Furthermore, the 200-year probability annual maximum flow in the 4-degree increase experiment was larger than the 900-year probability annual maximum flow rate in the past experiment, which is considered the largest class flood. Similar analysis results were obtained for the 109 primary river basins nationwide in Japan.

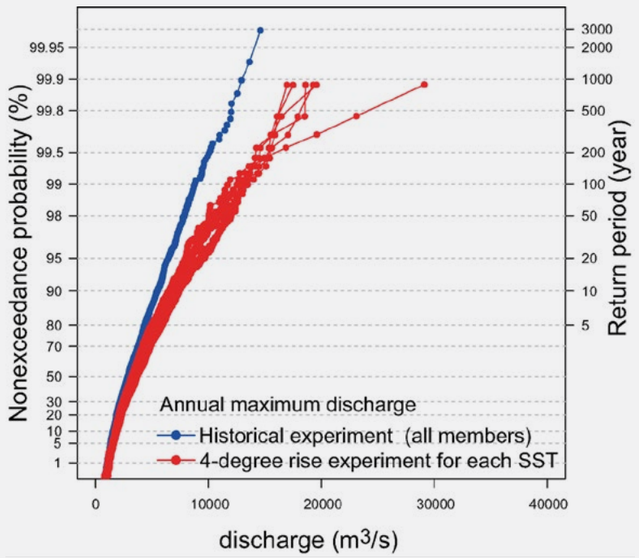

Figure 2: *Frequency distribution of annual maximum hourly flow in the Yodo River basin (Hirakata site). The blue line shows the probability plot for the past experiment, and the red lines show the probability plots for the 4-degree increase experiment (using scenario data with different sea surface temperatures) (from Tachikawa et al., 2017).*

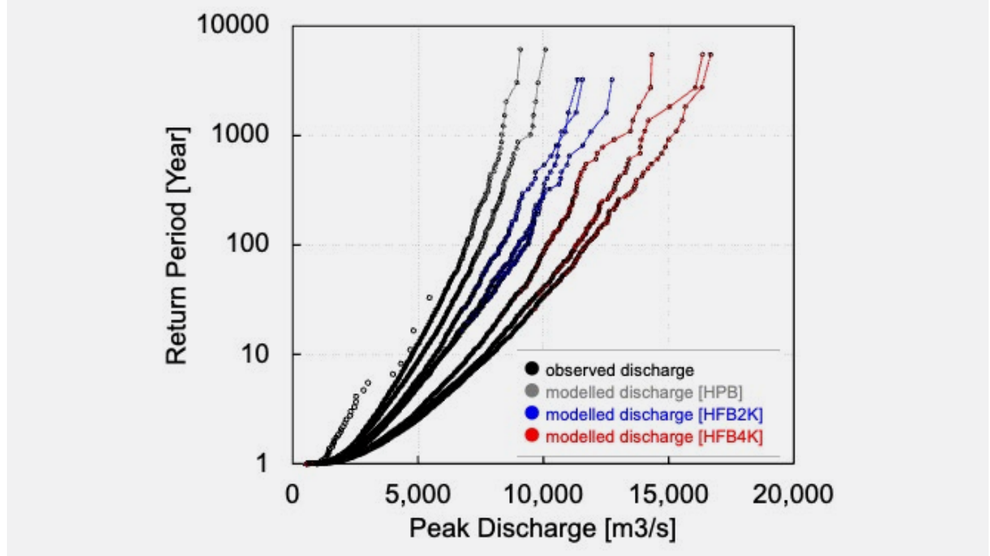

Figure 3: *Changes in the frequency distribution of annual maximum river discharge at the Nakhon Sawan (C2) site in the Chao Phraya River basin in Thailand. It shows differences between the historical experiment, 2-degree increase experiment, and 4-degree increase experiment (from Kato et al., 2022).*

Similar river flow prediction simulations were conducted for the Red River basin in China and Vietnam and the Chao Phraya River basin in Thailand. Figure 3 shows the analysis results for the Chao Phraya River basin. It was found that the annual maximum flow rate increases significantly with climate change. The rate of change of the annual maximum flow rate between the past experiment (corresponding to a 100-year return period) and the 2-degree increase experiment was 1.20 to 1.35 times, while the rate of change between the past experiment and the 4-degree increase experiment was 1.55 to 1.63 times. This indicates that flood risk increases in the Chao Phraya River basin and the Red River, similar to river basins in Japan.

A critical issue is to realize such a river flow change prediction for an arbitrary river basin and to predict flood risks. To achieve this, a rainfall-runoff simulation model that can be applied to any river basin is needed. To enhance prediction reliability, it is desirable to construct a rainfall-runoff model based on fundamental physical equations, where model parameters can be determined based on land cover, surface soil, and geological properties without requiring tuning. Although numerous studies have been conducted on this topic, it remains unresolved. It is necessary to develop a rainfall-runoff prediction model that can be applied to any river basin in the world, where standard model parameter values can be determined based on land cover, surface soil, and bedrock properties.

As part of this technological development, we developed a method to identify parameters for each land cover of the distributed rainfall-runoff model 1K-DHM using multiple sites and multiple flood events. This method was applied to the Kikuchi River basin in Kyushu Japan, confirming improved flood prediction accuracy. The parameter values identified based on Kikuchi River land cover data showed good reproducibility at many sites. Among 104 observation sites across fifteen basins in the Kyushu region used for verification, forty-one sites achieved a Nash coefficient between 0.5 and 0.8, and forty-seven sites achieved a coefficient of 0.8 or higher.

In addition to the land cover information, the accuracy of the distributed rainfall-runoff model 1K-DHM was further improved by incorporating soil distribution information into the distributed rainfall-runoff model. Figure 4 shows an example of the results. The reproducibility improved for the flow observation site on the Kikuchi River used in the parameter identification calculations. Furthermore, improved flow reproducibility was observed for observation sites with land cover and soil characteristics similar to those of the Kikuchi River basin. These results indicate that the potential to obtain parameter values with good reproducibility by using multiple observation site information with more diverse characteristics during parameter identification.

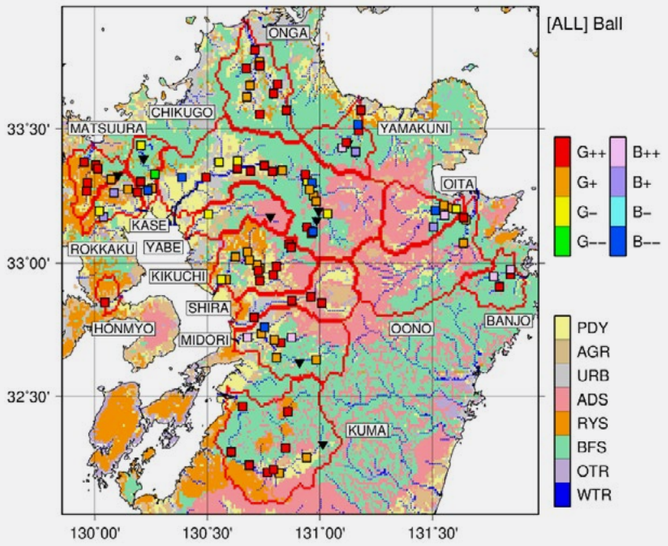

Figure 4: *Spatial distribution of soil information in the Kyushu region and the eight categories showing the improvement of Nash coefficients by reflecting the soil information. Squares along the river channel indicate observation points. Category classifications are shown for each point (from Kato et al., 2025).*

To enhance the accuracy of flood risk information, it is essential to simultaneously improve the input precipitation datasets and advance hydraulic simulation models capable of predicting floods and inundation in any river basin. As presented in this report, the fundamental approach to predicting flood risk lies in improving the accuracy of river flow predictions. High-resolution spatial information on topography, land cover, surface soil, and geology is becoming increasingly available. It is imperative to expedite the regional integration of rainfall-runoff simulation models using this information. A critical research challenge is developing a rainfall-runoff simulation model applicable to all river basins that can predict river flow at any location, enabling the prediction of river flow with a certain level of accuracy even in river basins lacking hydrological observation data.

The development of such risk information is not limited to Japan's river basins but applies to any river basin worldwide. Major flooding anywhere in the world would have a significant impact on the local socio-economy, which in turn would have an impact on Japan's socio-economy. In order to contribute to the prevention and mitigation of water-related disasters around the world, and to ensure that Japanese companies and Japanese citizens operating around the world are not affected by water-related disasters, it is necessary to develop flood prediction methods applicable to any river basin worldwide to generate water-related disaster hazard and risk information.

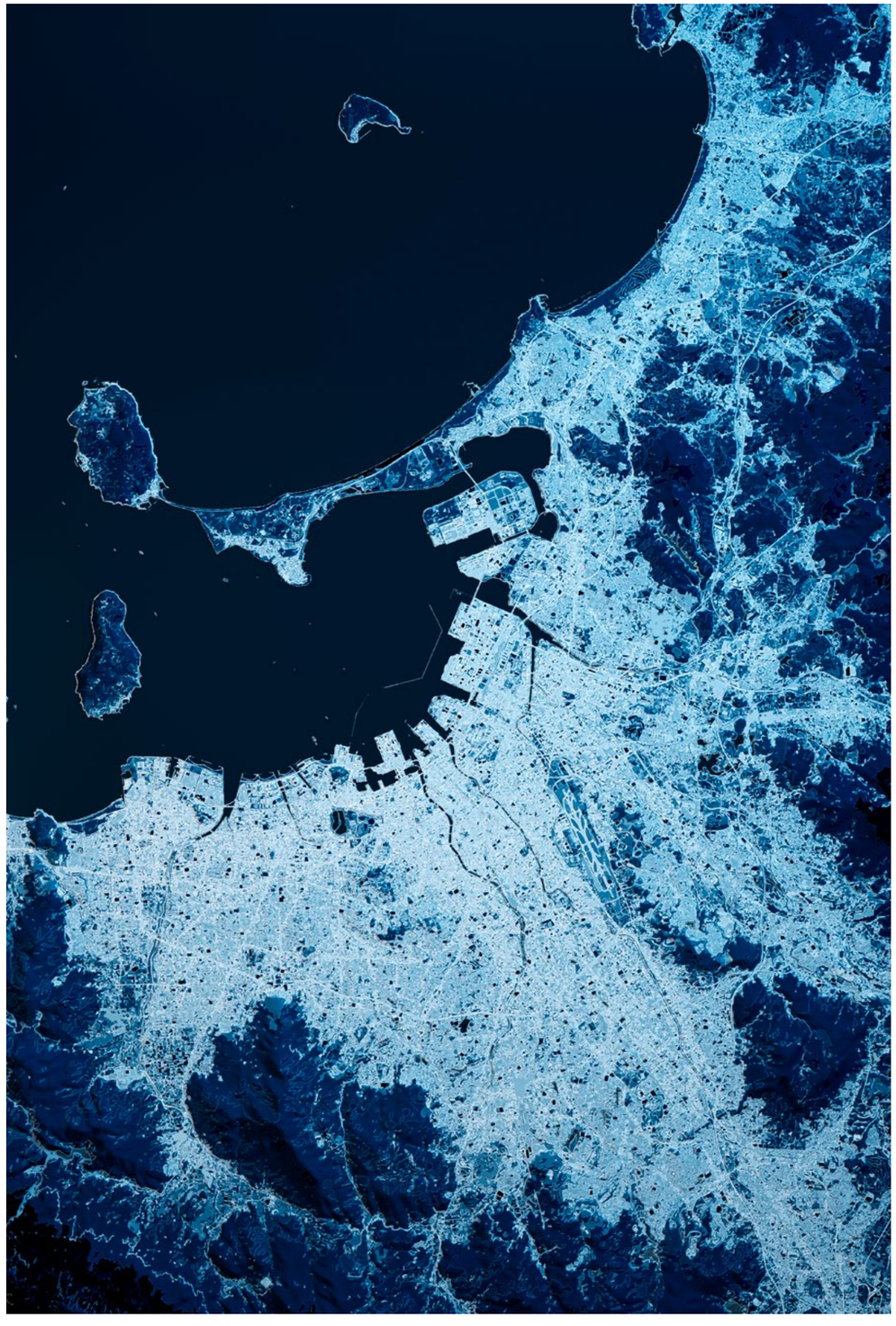

1.
Introduction

The Japan Meteorological Agency (JMA) has reported that the frequency and intensity of extreme heavy rainfall events are increasing every year and that global warming is affecting the occurrence of heavy rainfall events (Japan Meteorological Agency, 2025). The JMA also reports that the frequency and intensity of extreme heavy rainfall will continue to increase in the future. Many researchers and engineers are analyzing the effect of global warming on typhoons and the rainy season, as well as the effects of increased river flows and flooding and inundation caused by increased rainfall intensity.

The government is incorporating these scientific climate change prediction findings into flood control measures. The Japanese government has introduced the results of such scientific climate change prediction research into flood control measures, and is revising the river planning based on the assumption that short-term precipitation intensity will increase 1.15 times in Hokkaido and 1.1 times in other areas compared to the current situation (Ministry of Land, Infrastructure, Transport and Tourism, 2021). In response to this increase in external meteorological forces, the forecast information required for flooding has greatly expanded to include not only information on river flow and water levels at river locations, but also continuous information on river levels throughout the entire basin, the spread of flooding in urban areas, and the prediction of the behavior of flood waters that overflow river levees.

In response to these changes, science and technology for analyzing and predicting water-related disaster hazards have also changed significantly. The academic field that deals with the dynamics of water flow during floods is hydraulics, while hydrology deals with the physical mechanisms of the water cycle on a larger scale. Hydraulics deals with the analysis and prediction of river flow dynamics based on fluid dynamics. The design of river cross-sections that have the smallest cross-sectional area capable of carrying the largest flow, longitudinal channel design, and the design of dams and floodgates are fields traditionally addressed by hydraulics.

It also deals with sediment transport, not just water flow. Analyses of the hydrodynamic forces exerted on bridge piers and levees during floods, the mechanical mechanisms of sediment transport, and the impact of trees within rivers on flood flows remain important research topics today. Hydraulics also provides fundamental insights for river engineering that balances ecological environments for fish and aquatic life with river improvements for flood control and water utilization, alongside three-dimensional flow analysis.

On the other hand, hydrology aims to understand the water cycle and water balance occurring on the Earth's surface and near surface layers, including the atmosphere and trees, together with human activities and material cycles. It is an interdisciplinary field closely related to meteorology, climatology, agronomy, forestry, and limnology. It is offered as a fundamental subject in university lectures not only in engineering but also in the fields of science and agriculture. In the field of engineering, hydrology has developed as a field that provides fundamental information for rationally planning and designing social infrastructure facilities aimed at preventing and mitigating disasters caused by floods and droughts.

This ensures daily life remains unaffected even during extreme precipitation events (heavy rainfall or drought). Analyzing changes in the spatiotemporal patterns of precipitation during climate change and changes in the relationship between the frequency and intensity of floods and droughts are now important research topics in hydrology.

Currently, in addition to the design of the river channel, it is also necessary to predict the flood flow that cannot be carried by the river channel and will overflow the river levees and flood urban areas, to predict the spatial extent of the flooded area in the event of heavy rainfall exceeding the drainage capacity of the sewage system, and to predict damage to houses, agriculture, forestry, fishery, and commercial industries, as well as economic damage including the impact on distribution systems. In addition, it is necessary to forecast and provide information on damage to houses, agriculture, forestry, fisheries, and commerce, as well as economic damage, including the impact on logistics.

For this purpose, it is necessary to predict river flow based on rainfall forecast information, then to predict the situation where flooding occurs and spreads into urban areas when this flow exceeds the channel's discharge capacity, and then to link this to damage prediction. The entire watershed should be forecasted to generate hazard information, which can then be used to develop risk information to improve flood resilience in a comprehensive manner through a combination of hardware damage avoidance and mitigation measures, flood resilient urban development, and rapid livelihood restoration through property insurance. In addition, the combination of flood disaster resilience should be improved comprehensively.

Prediction of water disaster hazards encompasses two main categories: hazard prediction for planning purposes such as flood control planning, river improvement, urban development, and damage insurance, and real-time prediction that forecasts conditions while hazard events are in progress from time to time. Both types of prediction require essential technologies to forecast heavy rainfall and translate it into river flow information, urban flooding information, and ultimately risk information.

In the following sections, floods are discussed as a water-related disaster hazard, and flood prediction methods and the methods for predicting the risks are introduced. Section 2 describes the concepts of flood prediction and risk prediction that cause flood disasters, while Section 3 outlines the development history of flood prediction methods. Section 4 introduces research the authors have been involved in, analyzing examples from rivers in Japan and Southeast Asia to show how the relationship between the frequency and intensity of heavy rainfall and flooding may change due to global warming. Section 5 highlights current research by the authors aimed at improving the prediction accuracy of water-related disaster hazards and risks.

Finally, the above content is summarized, and future challenges are discussed to enhance disaster awareness and behavior change, thereby enhancing the disaster resilience of society.

2.
Prediction of Water Disaster Hazards and Risks

Water disasters such as urban flooding and flood inundations occur due to extreme precipitation, river flows, storm surges, or high waves. The heavy rain, floods, storm surges, and high waves that trigger these disasters are called water disaster hazards. They are sometimes referred to as natural external forces that cause water-related disasters. The occurrence of a hazard does not necessarily mean that a disaster will occur. Even if a large-scale flood inundation occurs, if no people live in the area and no social or economic activities are taking place, no damage will occur, and no disaster risk exists.

A disaster occurs when an extremely large natural phenomenon (hazard) strikes an area where social and economic activities are taking place, and the magnitude of that hazard exceeds the level of preparedness provided by hard measures like flood control facilities or soft measures like flood insurance. The relationship between the frequency and magnitude of damage caused, relative to the frequency and magnitude of water disaster hazard occurrence, is water disaster risk.

Predicting flood hazards in advance leads to predicting flood risks in advance. Flood hazard prediction includes planning-based prediction for developing flood control plans and real-time prediction. Planning-based prediction does not focus on predicting when the disaster will occur, but rather emphasize predicting the relationship between the frequency and magnitude of hazard occurrence.

To take flood control planning as an example, the objective is to define a precipitation period (ranging from a few hours to a few days in a river basin in Japan) related to the occurrence of floods for a reference point in a river, and to predict the amount of precipitation and magnitude of river flow that will occur once in a T-year period on average. On the other hand, real-time forecasting aims to predict precipitation intensity and river flow and water level several hours to several days ahead as the phenomenon progresses from time to time. When a disaster occurs is the key forecasting target. They are used to avoid damage in various activities, including the issuance of early warnings for evacuation and the management of flood control facilities.

2.1 Predicting the Relationship between Heavy Rainfall/ Flood Frequency and Intensity

The relationship between the frequency and intensity of heavy rain, such as obtaining the annual maximum 24-hour rainfall occurring on average in one hundred years, is the subject of analysis. This analytical method is called hydrological frequency analysis (e.g., Ikebuchi *et al.*, 2006; Shiiba *et al.*, 2013; Ministry of Land, Infrastructure, Transport and Tourism, Technical Standards for Rivers and Stream Erosion Control as of 2025). The analysis methods are standardized globally, and various analysis tools are packaged. Using the hydrological frequency analysis method, the relationship between the frequency and intensity of heavy rainfall events is obtained. A return period is defined as a safety level, and the magnitude of the heavy rainfall corresponding to that return period is determined. Subsequently, the flood that would be caused by that heavy rainfall is predicted. Using this information, flood control facilities are planned and constructed to prevent damage even if the flood defined here occurs.

The potential change in the frequency of heavy rainfall due to global warming has become a socially significant subject of analysis. Hydraulic structures designed to prevent floods and droughts are constructed based on a specific return period as a safety standard. It is essential information for social infrastructure development and non-life insurance management to clarify whether the safety standard set at the beginning of design will continue to function or not. For example, an analysis of the probability and statistical characteristics of hydrological quantities related to a hazard or risk, such as the possibility that a heavy rainfall that occurs in 100 years on average at present may occur once in 70 years on average due to global warming, is important information for the management of social infrastructure development and non-life insurance. This is because if the risk changes, appropriate countermeasures need to be developed in response.

For the 109 first class rivers in Japan, the design flood that forms the basis for flood control planning is defined by the government in the "Basic Policy for River Improvement," which is the government's policy for flood control projects. The flood level targeted to achieve this basic policy is called "basic high flood level". In order to realize this basic policy, the government formulates a "River Improvement Plan" that defines a specific implementation plan to be implemented over the next 20 to 30 years.

Flood control projects are then advanced nationwide according to these plans to maintain consistent flood control levels. The flood control safety level is set based on the return period of heavy rainfall. For rivers flowing through major metropolitan areas, such as the Tone, Arakawa, Yodo, Kiso, and Chikugo Rivers, the government has set a 200-year return period as the flood control safety level, and the flood caused by such heavy rainfall is designated as the "basic high flood level". The return period is determined considering the population and assets within the river basin, and in the case of the first-class rivers, the recurrence period is set at 100 to 200 years.

The method for determining the basic high flood level is described in the Ministry of Land, Infrastructure, Transport and Tourism's Technical Standards for Rivers and Sediment Control, Planning Section (as of August 2025). First, a design rainfall is set. This is then used as input data in a rainfall-runoff model to calculate the river flow at the target location. If the flood control level is set to the level corresponding to two hundred years of heavy rainfall, we need time series data of two hundred years of heavy rainfall as the rainfall data for hydraulic engineering planning.

However, such precipitation observation data generally does not exist. Precipitation observations in Japan began in 1875, and even the longest observation period for precipitation data is only 150 years at most. Therefore, rainfall time series data (design rainfall) with a 200-years return period is generated by extrapolation using probabilistic statistical methods.

Recently, climate models have generated precipitation time series simulation data equivalent to several thousand years. Using this data, it has become possible to generate a design rainfall of the 200-year return period directly from the generated data itself, without using a conventional probabilistic statistical model. Once the design rainfall is determined, it is used as input data for a rainfall-runoff model to calculate river discharge. The rainfall-runoff model is a simulation model that uses precipitation data as input to calculate river flow at the target location, and its accuracy is key to estimating hazards and risks.
Section 3 introduces representative rainfall-runoff models.

2.2 Real-Time Forecasting of Heavy Rainfall and Flooding

Real-time flood forecasting involves providing flood prediction information for the next few hours or days as heavy rain progresses. In Japan, the Japan Meteorological Agency (JMA) distributes real-time hazard information for flood and sediment disasters, such as basin rainfall indices, surface rainfall indices, and soil rainfall indices, at a spatial resolution of 1 km across the entire country. This service is named "Kikikuru (Hazard Distribution)" and is available at https://www.jma.go.jp/bosai/risk/. The basin rainfall index and soil rainfall index use precipitation data as input. They calculate river flow and soil moisture using the tank model, one of the rainfall-runoff models, and express the relative risk of flood disasters and landslides using these values as indicators. These indicators are also used as criteria for issuing warnings and advisories.

The Basin Rainfall Index is an indicator calculated from precipitation data and is not directly comparable to physical flow rates or water levels. However, its values correspond to flow calculations derived from a rainfall-runoff model and have been shown to correlate well with observed water levels (Japan Meteorological Agency, Atmosphere and Ocean Department, Meteorological Risk Management Division, 2023).The Soil Rainfall Index represents the soil moisture in the tank model calculated at 1 km spatial resolution, indicating how much rainwater is contained within a hillside slope.

The Ministry of Land, Infrastructure, Transport and Tourism (MLIT) predicts river levels for flood forecast rivers and distributes information on the risk of overflows for each river section in real time using "Flood Risk Line, https://frl.river.go.jp/". It uses the river flow discharge obtained from a rainfall-runoff model as the upstream flow for the target river section and forecasts river water levels in real time. Previously, the "Flood Warning Risk Distribution (Flood Kikkuru)" was provided by the JMA and the "Flood Risk Line" provided by the MLIT were each available on separate websites. However, starting in February 2023, it became possible to access this information integrated on the JMA's Flood Kikikuru web site.

2.3 From Flood Hazard Prediction to Flood Risk Prediction

Both for planning purposes and real-time forecasting, the expected information is becoming more sophisticated from hazard forecasting to risk forecasting. Flood hazard maps have traditionally been created by simulating flood inundation under scenarios of the maximum anticipated scale (1000-year return period) and planning scale (50- to 200-year return periods), then mapping the extent of the inundated areas. In addition to these maps, multi-level maps showing the extent and depth of inundation under more frequent rainfall scenarios (10-year, 30-year, 50-year) have been prepared and are now available to the public for use in urban planning and residential planning.

Based on these inundation zone maps, information necessary for risk assessment and mitigation such as analyzing affected areas and populations, estimating damage costs, and securing evacuation routes, is also being generated. Typical websites providing flood hazard and risk information created using rainfall-runoff models for river flow prediction and flood analysis are listed here.

Flood Risk Map
(Flood Frequency Map) and Multi-Stage Flood Scenario Maps by Rainfall Intensity (River Sections Managed by the Ministry of Land, Infrastructure, Transport and Tourism)
https://www.mlit.go.jp/river/kasen/ryuiki_pro/risk_map.html

Flood Risk Map
(Flood Frequency Map) and Multi-Stage Flood Scenario Maps by Rainfall Intensity (River Sections Managed by Local Governments) Example: Osaka Prefecture Flood Risk Display Map
https://www.river.pref.osaka.jp/

Hazard Map Portal Site
(Links to flood hazard maps created by national and local governments)
https://disaportal.gsi.go.jp/

For real-time flood prediction information, Kikikuru introduced in the previous section displays risk levels on a 5-point scale and is used for issuing warnings.

Kikikuru
(Flood risk level distribution)
https://www.jma.go.jp/bosai/risk/

Water Disaster Risk Line
https://frl.river.go.jp/

Based on the recommendations of the Task Force on Climate-related Financial Disclosures (TCFD), the MLIT has not only to disclosed risk information to residents, but also to the private sector, by preparing "A guide to flood risk assessment for enhanced TCFD disclosures," https://www.mlit.go.jp/river/shinngikai_blog/tcfd/index.html.Risk information may include a variety of information other than those listed above.

2.4 Challenges in Flood Hazard Prediction

Accurate prediction of river discharge is fundamental to achieving nationwide flood forecasting and related risk prediction. Rainfall-runoff simulation models are used for river discharge prediction, converting precipitation data into river flow. In order to improve the prediction accuracy, it is necessary to appropriately define the structure of the rainfall-runoff simulation model and the flow characteristic values (model parameters) that govern the behavior of rainwater in the model.

The model parameter values are considered to be related to the characteristics of the land cover, surface soil, and base rock. However, due to the model structure of rainfall-runoff simulation models and the spatial resolution of the simulation model, it is not easy to incorporate the hydraulic properties obtained from soil samples measured in the field into the simulation model.

Although data capturing the spatial distribution of surface soils and basement rocks are now available, there is no geographic information data showing the three-dimensional distribution of soils and basement rocks extending below the ground surface. In addition, the soil samples measured in the field are only soil samples at a specific point in a river basin, and the hydraulic parameters obtained from them are not model parameter values that represent the average hydraulic properties representative of the spatial extent of the soil and basement rock.

Numerous studies have been conducted worldwide to achieve flood forecasting in rivers with inadequate observational information by determining the values of model parameters from external data such as land cover, soil, and base rock, instead of tuning and identifying them from hydrological observation data. However, no effective method has yet been established.

Developing a rainfall-runoff simulation model applicable to any river basin is fundamental research underpinning flood hazard and risk prediction. In the joint research with Tokio Marine Research Institute, Inc. introduced in Section 5, we are advancing research to rationally determine the model parameter values for a physical rainfall-runoff model.

3.
Development History of Flood Runoff Prediction Methods

To predict flood hazards and associated risks, rainfall-runoff simulation models that convert precipitation intensity into river flow are essential. Numerous studies on the observation and modeling of rainfall-runoff phenomena have been conducted in Japan since the 1950s. Various efforts have been made to improve the accuracy of rainfall-runoff models in line with the increasing demand for information on flood hazard and risk (*e.g., Ikebuchi et al.,2006; Shiiba et al., 2013); MLIT, Technical Standards for Rivers and Sediment Control*).

3.1 Rainfall-Runoff Systems and Modeling

Precipitation that reaches mountain slopes, agricultural lands, and urban areas flows out to rivers through various pathways and then to the sea. The process is shown schematically in Figure 1. This figure shows the process of rainwater conversion from precipitation to river flow as a combination of subsystems and their interconnectedness with inputs and outputs. The squares indicate subsystems, the circles indicate inputs or outputs, and the arrows indicate the direction of inputs or outputs. Key physical quantities characterizing the system include inputs, outputs and system parameters.

A rainfall-runoff model is a mathematical model that expresses these subsystems in mathematical equations and interconnects them to convert a rainfall time series into a river discharge time series. To construct a rainfall-runoff model, the entire watershed is usually divided into appropriate sizes based on the watershed topography as shown in Figure 2. The rainfall-runoff system is modeled in each divided watershed, and the entire rainfall-runoff system is modeled by interconnecting them.

Inputs:
External causes acting on the system (e.g., precipitation)

Outputs:
Results generated by one or more inputs acting on the system (e.g., river flow)

System Parameters:
Parameters governing the system's dynamic characteristics (e.g., parameters determined by topography or characterizing surface and subsurface rainfall flow)

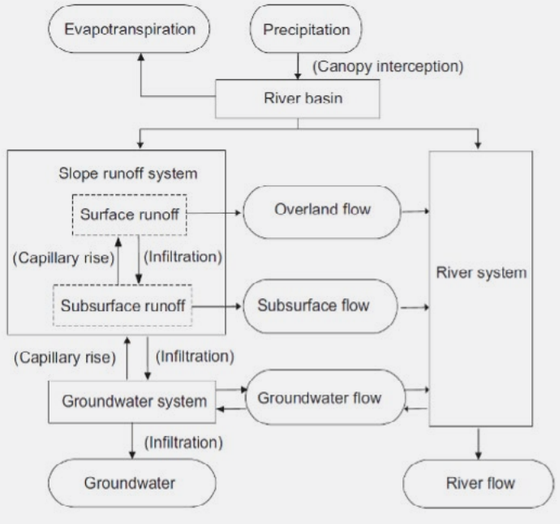

Figure 1: *Rainfall-runoff system (from Kanamaru and Takasao, 1975).*

Rainfall-runoff models are broadly classified into conceptual rainfall-runoff models that conceptually represent the flow and storage of rainwater and physical rainfall-runoff models that attempt to represent these hydrological processes as physically as possible.

Section 3.2 discusses the tank model as a representative conceptual model. Section 3.3 introduces a distributed rainfall-runoff model, which aims to incorporate spatial physical information of the river basin into the simulation model.

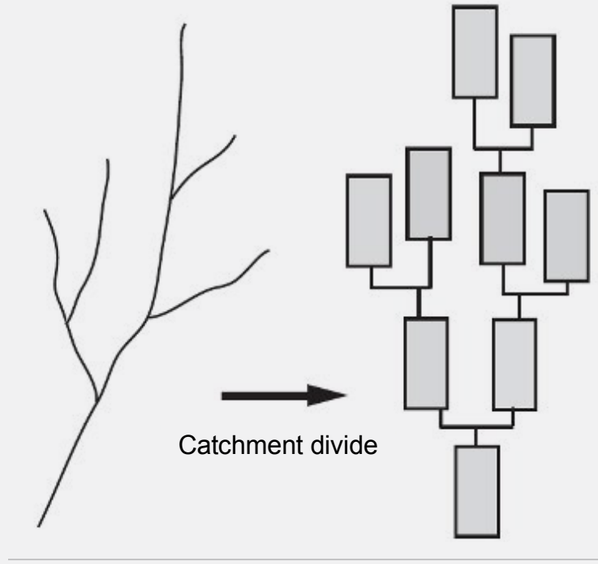

A) Catchment division according to river channel classification.

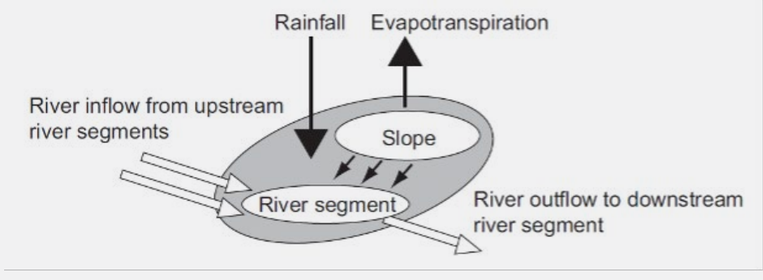

B) Movement of rainwater and river runoff in a subdivided basin.

Figure 2: *River basin segmentation (top) and modeling of stormwater flow in segmented basins (bottom).*

3.2 Conceptual Rainfall-Runoff Models

A typical conceptual model is the tank model. It has been applied in many cases ranging from flood forecasting for a few days to river flow forecasting throughout the year. The basic structure of the tank model is shown in Figure 3. Outflow holes are set at the side and bottom of the tanks, which are arranged in series to reproduce runoff.

The tank model represents groundwater discharge within its structure, and precipitation and, in the case of long-term extraction forecasts, evapotranspiration are given as input data. The tank model can be composed of countless combinations of tank arrangement, number of tanks, number of outfalls, and so on.

In Japan, a four-tank model is often used, as shown in Figure 3. Conceptually, lateral outflow from the upper tank is considered as surface runoff, outflow from the upper tank to the lower tanks is considered as infiltration into the lower layer, and lateral outflow from the lower tank is considered as groundwater outflow.

The basin rainfall index, surface rainfall index, and soil rainfall index calculated by the JMA in Kikikuru cover the entire country of Japan with a grid of approximately 1 km squares. Within each grid cell, a three-tier and a five-tier tank model in series is applied (JMA Atmosphere and Ocean Department, Meteorological Risk Management Division, 2023).

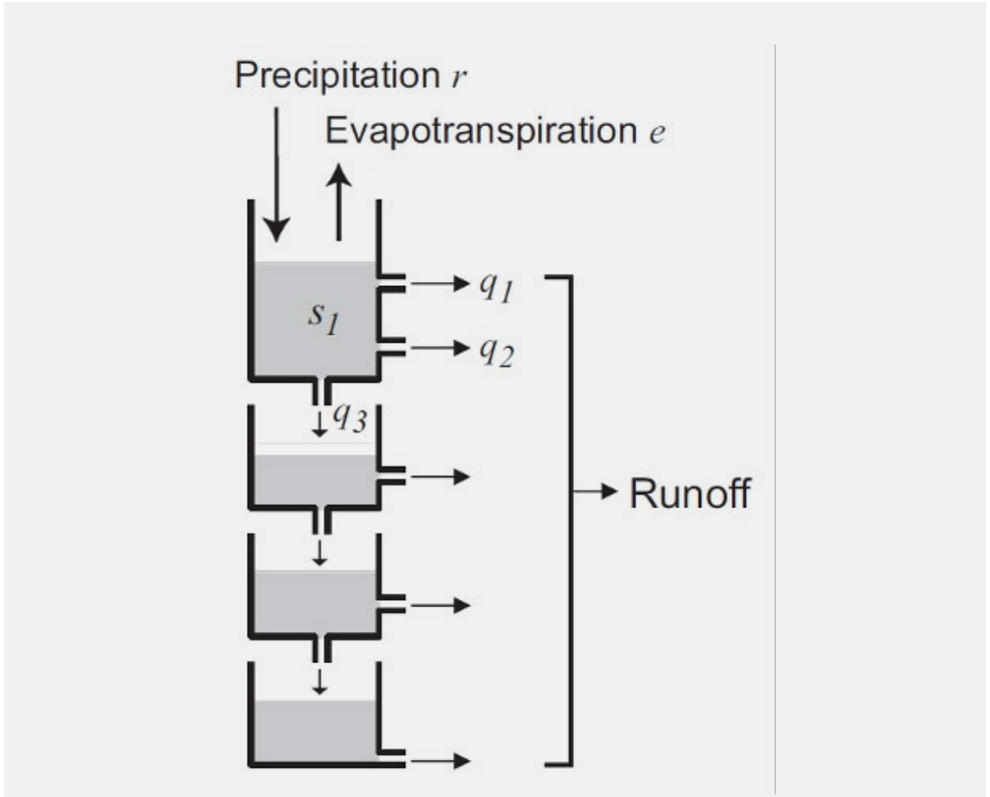

Figure 3: *Structure of the tank model.*

3.3 Distributed Rainfall-Runoff Model Incorporating Spatial Distribution Information

A distributed rainfall-runoff model is designed to directly incorporate geographic information such as topography, land cover, surface soil, and geology, along with spatially distributed information like radar precipitation data. The structure of a typical distributed rainfall-runoff model is shown in Figure 4. A commonly used distributed rainfall-runoff model employs elevation data from a grid covering the entire country such as National Land Digital Information. It assumes rainwater flows in the direction of the steepest direction from each grid point, defining the flow direction one-dimensionally to route the water flow.

The 1K-DHM model described in the next chapter is also a runoff model of this type. By introducing model parameters that can be related by topography, land cover, and surface soil into the equation for calculating rainwater flow, the model is oriented to determine the model parameter values from spatial geographic information such as land cover and surface soil information without tuning the model parameters. In contrast to simulation models like the tank model that conceptually represent rainwater flow, this model is sometimes called a physically distributed rainfall-runoff model.

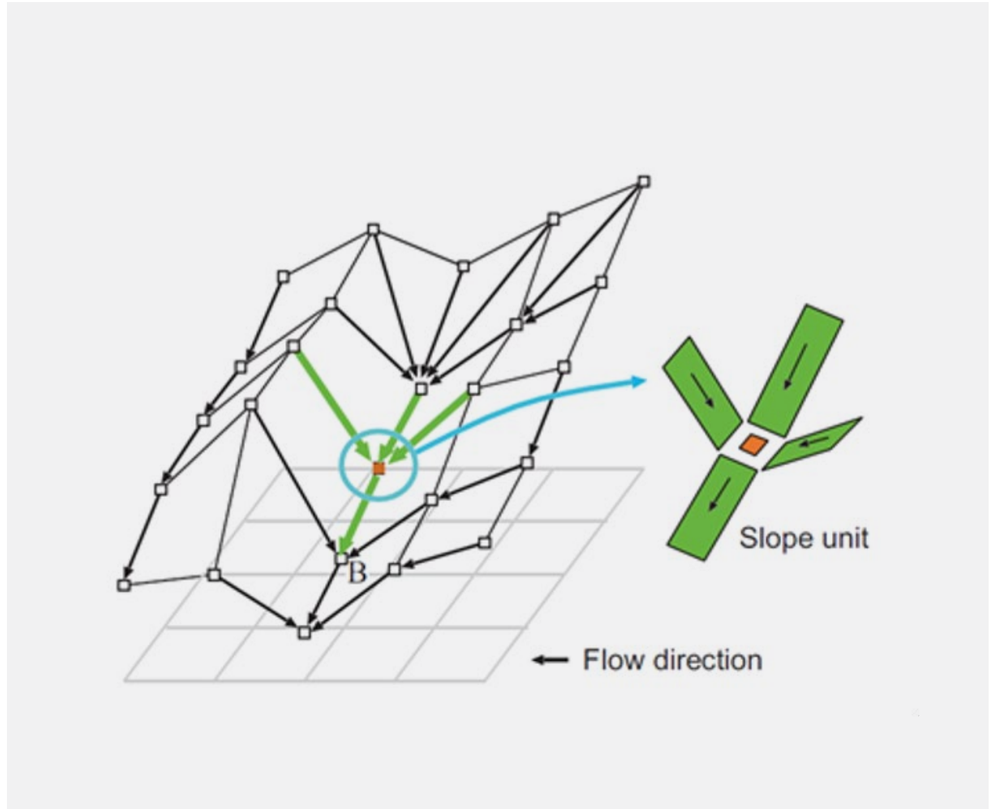

Figure 4: *Watershed topography representation using digital elevation data and its use in distributed rainfall-runoff modeling.*

3.4 Rainfall-Runoff-Inundation Model for Integrated Prediction of River Flow, Flooding, and Inundation

Flooding occurs when the intensity of heavy rainfall in urban areas exceeds the drainage intensity of the sewage system. Furthermore, if the flood generated by heavy rainfall exceeds the discharge capacity of a river, the floodwater overflows the banks and spreads over urban areas. To predict the spread of floodwater in urban areas, a rainfall-runoff model is usually used to predict river discharge. This flow is then fed into a river flow model as boundary conditions to calculate flood discharge in the river.

Next, assuming overtopping occurs at points where the river flow exceeds the carrying capacity, the amount of overflow is given to a two-dimensional flood flow model to predict the behavior of floodwater flowing through an urban area. Recently, simulation models that solve rainfall-runoff in the watershed, flood flow in the river, and inundation flow in the floodplain as an integrated system have been developed and are widely used (e.g., the Rainfall-Runoff-Inundation (RRI) model (Figure 5) and DioVISTA/Flood).

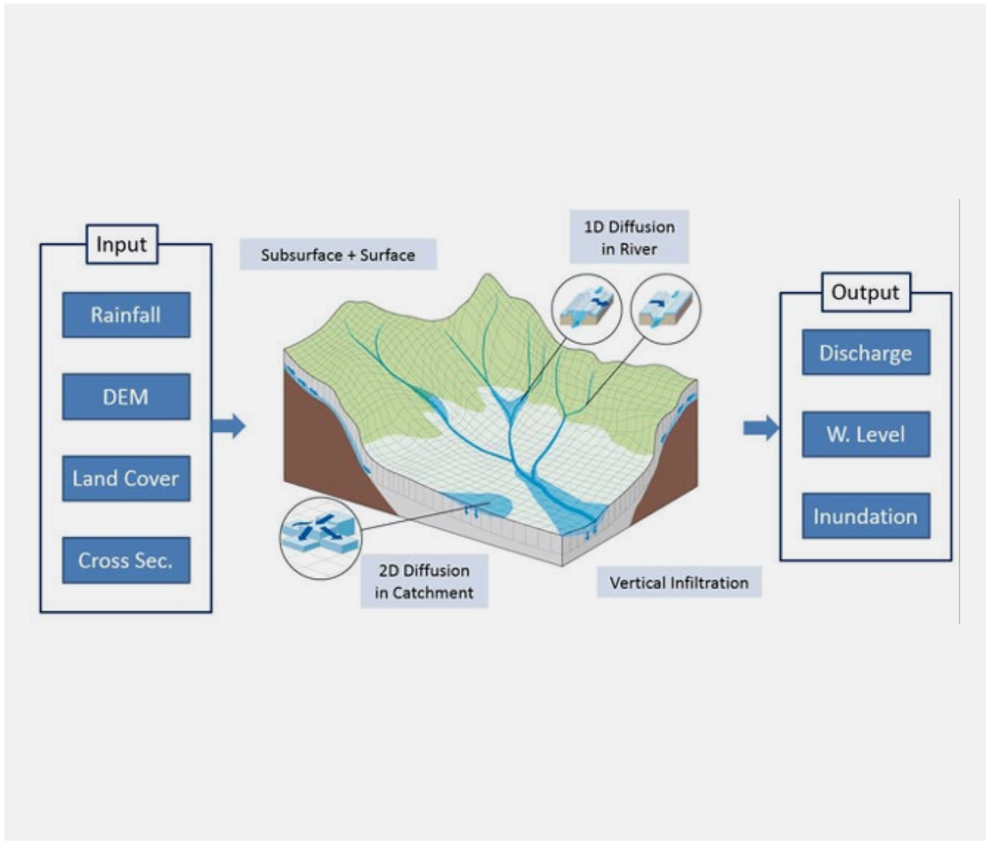

Figure 5: *Structure of the RRI model (International Center for Water Hazard and Risk Management (ICHARM), Public Works Research Institute, https://www.pwri.go.jp/icharm/research/rri/index.html).*

3.5 Role and Challenges of Rainfall-Runoff Models

Flood forecasting for flood risk assessment targets floods with return periods exceeding several hundred years. If flow time series data exceeding several hundred years are available, statistical analysis of that data could predict the magnitude of rare floods such as those with a 200-year return period. However, such observed flow data does not exist. Therefore, it has been common practice to use hydrological frequency analysis methods to generate rainfall time series data corresponding to the design return period.

This simulated data is then input into a rainfall-runoff model to obtain high flood flows of rare magnitude. Recently, climate prediction models have been used to generate long-term climate information databases that cover thousands of years such as the "Database for Policy Decision making for Future climate change (d4PDF)" developed by the Meteorological Research Institute (Mizuta *et al.*, 2017). Using the precipitation data from the databases, it has become possible to predict flood data corresponding to return periods of several hundred years.

d4PDF (https://www.miroc-gcm.jp/d4PDF/index_en.html) is a climate prediction dataset generated through climate prediction experiments using the MRI-AGCM3.2 global atmospheric model developed by the Meteorological Research Institute with a horizontal resolution of approximately 60 km and regional experiments using the NHRCM regional climate model covering the area around Japan with a horizontal resolution of approximately 20 km. The global model experiments consist of past experiments, non-warming experiments, 1.5 degree increase experiments, 2 degree increase experiments, and 4 degree increase experiments. The regional model experiments consist of past experiments, 1.5 degree increase experiments, 2 degree increase experiments, and 4 degree increase experiments.

A unique feature of the experiments is that a large number of ensemble experiments were conducted to allow for the prediction of changes in the frequency and intensity of extreme events. For example, the 4 degree increase experiments using the regional model generated a total of 5,400 years of climate simulation data, enabling the analysis of changes in extreme hydrological variables such as annual maximum daily rainfall in probability distributions.

Using the precipitation dataset included in this dataset, it is possible to generate very long-term river discharge data using a rainfall-runoff model and to quantitatively analyze rare flood events to estimate water-related disaster risks. d4PDF makes it possible to analyze changes in flood discharge due to global warming as changes in frequency distributions, such as annual maximum flood discharge. This is an extremely important development for predicting changes in water-related disaster risk.

To achieve this, a rainfall-runoff model that can be applied to any river basin is needed. To increase the probability of prediction, it is desirable to use a rainfall-runoff model that consists of physical basic equations, and the model parameter values used in the model can be determined based on land cover, surface soil, and geological properties without tuning. Many such studies have been conducted but have yet to be resolved. It is necessary to develop a rainfall-runoff prediction model that can be applied to any river basin in the world, and to develop standard values for model parameters based on the physical properties of land cover, surface soil, and base rock.

Subsequent chapters will introduce the work our team has undertaken on these challenges, focusing on collaborative research with Tokio Marine Research Institute, Inc.

4.
Projecting Changes in Flood Hazard Intensity and Frequency Due to Climate Change

Using precipitation datasets created with d4PDF, we predicted flood discharge for major river basins in Japan. Next, we analyzed how hydrological extremes, such as annual maximum peak discharge, might change under climate warming scenarios as shifts in probability distributions.

4.1 Changes in Annual Maximum Precipitation and Annual Maximum Peak Discharge in Major Japanese Rivers

Targeting major river basins in Japan, we analyzed future changes in the probability distribution of extreme flood discharge for the Ara, Shonai, and Yodo river basins using precipitation data obtained from d4PDF (Tachikawa *et al.*, 2017). First, we analyzed future changes in the frequency distribution of extreme precipitation amounts. Next, using a rainfall-runoff model, we analyzed future changes in the frequency distribution of extreme flow rates and examined flow rates equivalent to a 1000-year return period.

4.1.1 Structure of the Distributed Rainfall-Runoff Model 1K-DHM

The distributed rainfall-runoff model 1K-DHM (https://hywr.kuciv.kyoto-u.ac.jp/products/1K-DHM/1K-DHM.html), developed at the Graduate School of Engineering, Kyoto University (Department of Civil and Earth Resources Engineering, Hydrology and Water Resources Laboratory), was used. This rainfall-runoff model is a distributed rainfall-runoff model using digital elevation data with a spatial resolution of 30 seconds (approximately 1 km grid). It calculates river discharge from precipitation data using a kinematic wave model that accounts for both surface and sub-surface runoff.

Figure 6 shows the spatial model structure of 1K-DHM. For each 1 km grid cell, a river is placed at its center with rectangular slopes on both sides to model the watershed topography. Within the slope areas of each grid cell, rainfall intensity is converted into runoff rate. In the river sections, lateral inflow from both slopes and inflow from upstream grids are obtained to calculate the outflow to the downstream grid cell. The flow direction for rivers within each grid cell is set as the steepest gradient direction among the adjacent eight grid cells. River flow is then calculated sequentially from upstream to downstream.

Elevation and flow direction data for constructing the watershed topography model utilized digital topography data from HydroSHEDS (https://www.hydrosheds.org/), a hydrological topography database covering all terrestrial areas of the Earth. Input precipitation data consists of two-dimensional spatial distribution data covering the target watershed. The two-dimensional spatial rainfall data closest to the center coordinates of each topography grid cell is selected and assigned to that grid cell.

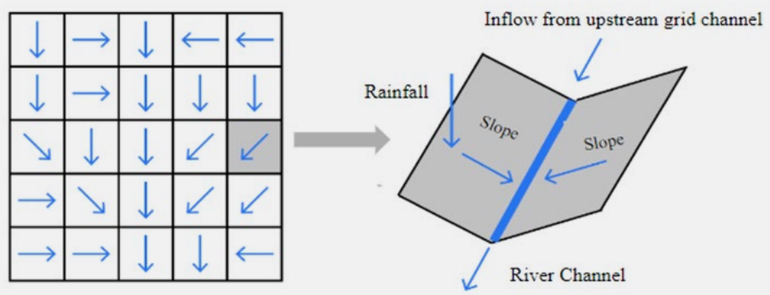

A) Determination of flow direction using digital elevation data and a watershed model within a single grid cell.

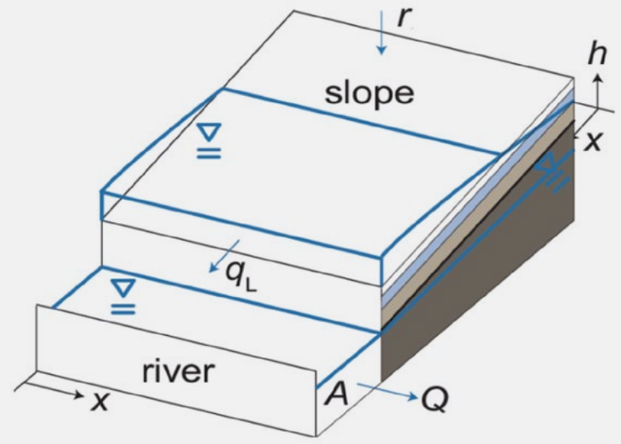

B) Slope flow model and river flow model within topography grid cells.

Figure 6: *Modeling of basin topography and flow in the 1K-DHM.*

4.1.2 Modeling of Rainfall-runoff processes

For river flow, the kinematic wave model (Shiiba *et al.*, 2013)

$$\frac{\partial A}{\partial t}+\frac{\partial Q}{\partial x}=q_L \qquad (1)$$

$$Q=\alpha_c A^m \qquad (2)$$

is used, where t is time, x is distance, A is cross-sectional area, Q is discharge, q_L is lateral inflow per unit length along the flow direction, α_c is a parameter $\alpha_c=(1/B_c)^{2/3}\sqrt{i_c}/n_c$, i_c is channel slope, n_c is channel roughness coefficient, B_c is channel width, and m is a constant (=5/3). For slope flow, the kinematic wave model considering unsaturated and saturated runoff in the soil layer and surface runoff expressed as

$$\frac{\partial h}{\partial t}+\frac{\partial q}{\partial x}=r-e \qquad (3)$$

$$q(h)=\begin{cases} v_c d_c\left(\frac{h}{d_c}\right)^{\beta} & , \quad 0\le h<d_c \\ v_c d_c+v_a(h-d_c) & , \quad d_c\le h<d \\ v_c d_c+v_a(h-d_c)+\alpha(h-d)^m & , \quad d\le h \end{cases} \qquad (4)$$

where, h is the runoff height, q is the slope runoff per unit width, r is the precipitation intensity, e is the evapotranspiration intensity, dc is the pore thickness in the soil matrix, d is the total pore thickness in the soil, α_s is the parameter $\alpha_s=\sqrt{i_s}/n_s$, i_s is the slope gradient, n_s is the equivalent surface roughness, m is the constant (=5/3), k_c is the saturated hydraulic conductivity of the soil matrix layer, k_a is the hydraulic conductivity of the saturated flow layer, and $vc = k_c i$, $v_a=k_a i$, $k_c= k_a/\beta$. The slope gradient i is determined by topographic data. the d_c, d, n_s, k_c, k_a *and* β are model parameters that take different values depending on land cover and surface soil type.

These parameter values are generally determined to ensure that observed flow rates match calculated flow rates. Developing a method to establish these values based on topography and soil/geological information rather than tuning them and applying it to any river basin with insufficient hydrological observation data is a globally significant research challenge.

4.1.3 Analysis Results of Future Changes in Frequency Distributions of Extreme Precipitation and River Discharge

We constructed the distributed rainfall-runoff model 1K-DHM for Japan's major river basins: the Ara River basin (2,940km^2), the Shonai River basin (1,010km^2), and the Yodo River basin (8,240km^2). The basin topography models for the study basins are shown in Figure 7.

The ensemble climate prediction database d4PDF (https://www.miroc-gcm.jp/ d4PDF/) consists of hourly time series data totaling 3,000 years from 50 ensemble members, with each member representing 60 years of the past experiment calculations, and hourly time series data totaling 5,400 years from 90 ensemble members, with each member representing 60 years of the 4-degree increase experiment calculations. We confirmed the reproducibility of extreme precipitation events in these datasets. Next, we analyzed changes in the frequency distribution of extreme precipitation due to global warming.

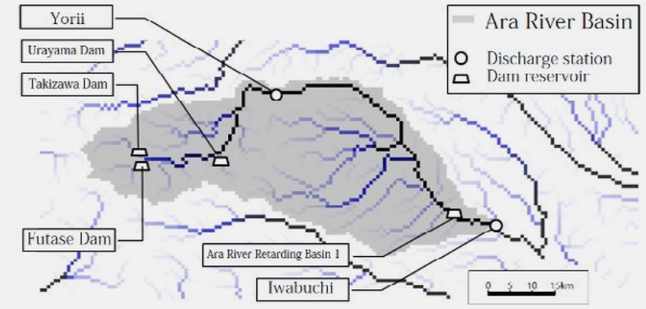

A) Arakawa River basin (Upper Iwabuchi Station).

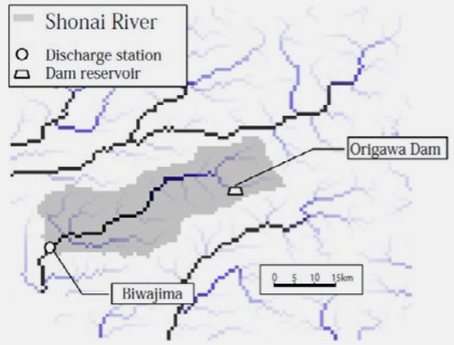

B) Shonai River basin (Upper Biwajima Station).

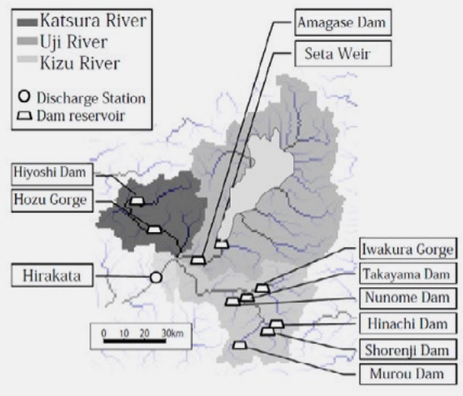

C) Yodo River basin (upstream of Hirakata Station).

Figure 7: *Study basins (from Tachikawa et al., 2017).*

Figure 8 shows probability plots (relationship between annual maximum values and non-exceedance probability (left vertical axis) and return period (right vertical axis)) for annual maximum 24-hour and 72-hour rainfall data from past experiments (three thousand years) and six 4 degree increase experiments with different sea surface temperatures (nine hundred years for each experiment). Each figure also includes probability plots of annual maximum values derived from observed data. The red lines in Figure 8 represent the six probability plots from the 4-degree increase experiments with different projected sea surface temperatures. All probability plots for the 4-degree increase experiment are to the right of those in blue for the past experiment.

The results show an increase in extreme precipitation due to global warming regardless of sea surface temperature. The 200-year annual maximum precipitation in the 4 degree increase experiments increased by 1.2 to 1.4 times compared to the past experiment. Furthermore, the 200-year annual maximum precipitation of the 4-degree increase experiment and the 900-year annual maximum precipitation of the past experiment were almost the same. This is a result that should be noted because it indicates that values that are normally considered unlikely to occur at the current maximum class scale will increase in frequency to the level of flood control planning with a 200-year return period at the time of a 4-degree increase.

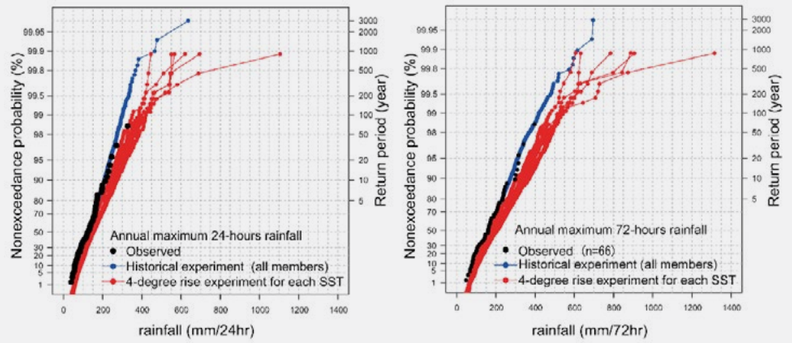

A) Ara River basin.

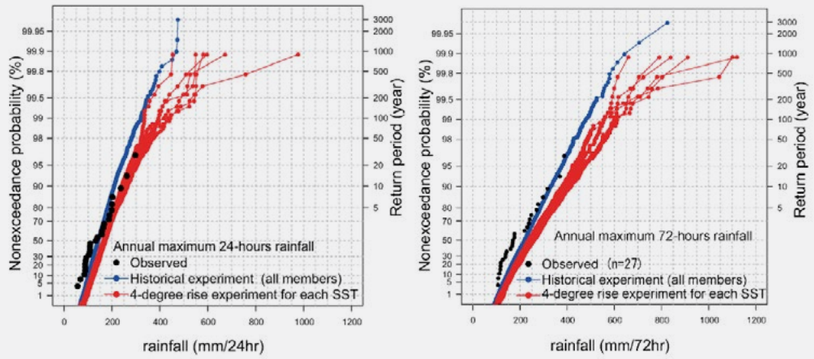

B) Shonai River basin.

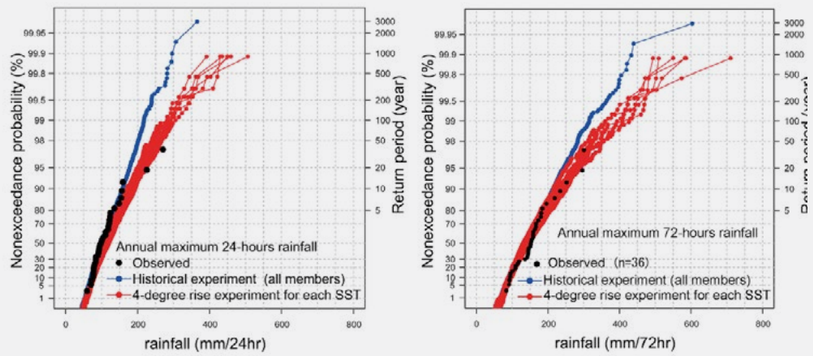

C) Yodo River basin.

Figure 8: *Probability plots showing the annual maximum 24-hour precipitation (left) and annual maximum 72-hour rainfall (right) for each basin. Black dots indicate observed rainfall, blue lines represent past experiments, and red lines indicate the 4-degree increase experiment (probability plots for each SST setting) (from Tachikawa et al., 2017).*

Using these rainfall data, we performed rainfall-runoff calculations and obtained annual maximum hourly discharge data for 3,000 years of the past experiment and 5,400 years of the 4-degree increase experiment. A probability plot of the annual maximum flow obtained using them is shown in Figure-9. The annual maximum probability discharge in the 4-degree increase experiments was larger than that in the past experiment for all sea surface temperature patterns, and the increase rate was greater as the non-exceedance probability increased. Comparing the 200-year annual maximum discharge between the past experiment and the 4-degree increase experiment, all three basins showed increases ranging from 1.5 to 1.7 times.

The increase rate for annual maximum precipitation was 1.2 to 1.4 times, meaning the increase rate for annual maximum discharge was greater than that. Generally, as rainfall intensity increases, flood peak discharge shows a larger increase rate above a certain rainfall intensity. This likely reflects the inherent nonlinearity of actual rainfall-runoff phenomena represented by the rainfall-runoff model, causing the annual maximum flow increase rate to exceed that of the annual maximum precipitation. Furthermore, the 200-year annual maximum flow rate in the 4-degree increase experiment exceeded the 900-year annual maximum flow rate from the past experiment. The result should be considered to discuss future flood control planning.

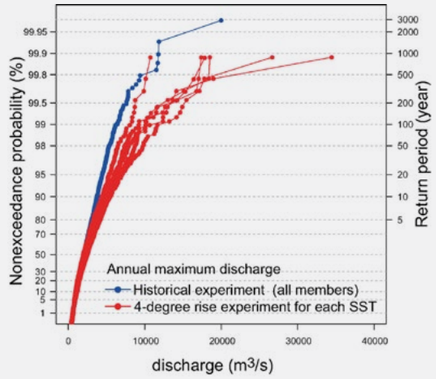

A) Arakawa River basin (Iwabuchi Station).

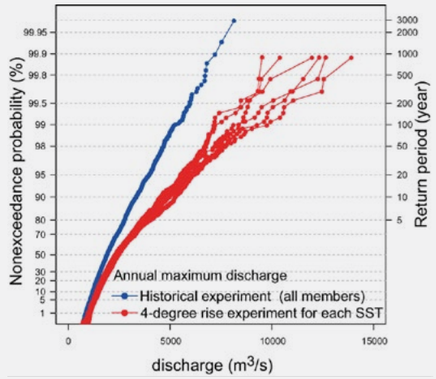

B) Yodo River basin (Hirakata Station).

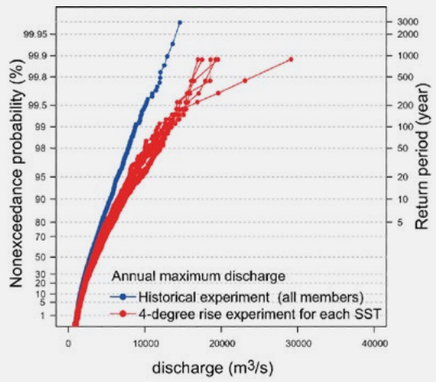

C) Yodo River basin.

Figure 9: *Probability plots showing the annual maximum 24-hour precipitation (left) and annual maximum 72-hour rainfall (right) for each basin. Black dots indicate observed rainfall, blue lines represent past experiments, and red lines indicate the 4-degree increase experiment (probability plots for each SST setting) (from Tachikawa et al., 2017).*

4.1.4 Summary and Discussion
We analyzed changes in the frequency distribution of annual maximum hourly discharge estimated with a distributed rainfall-runoff model using d4PDF precipitation data as input. The following results were obtained for the three study basins:

1) The frequency distributions of annual maximum 24-hour precipitation obtained from observations and the d4PDF past experiment showed good agreement at non-exceedance probabilities of 0.95 or lower.

2) For the 4-degree increase experiment, the 200-year annual maximum 24-hour precipitation in all three basins was 1.3 to 1.4 times that of the past experiment, while the one of the annual maximum hourly discharge was 1.5 to 1.7 times greater. The larger increase relative to the annual maximum 24-hour precipitation is thought to be the result of the inherent nonlinearity of the actual rainfall-runoff phenomenon represented by the rainfall-runoff model.

3) The 200-year annual maximum precipitation in the 4-degree increase experiment was nearly the same as the 900-year annual maximum precipitation in the past experiment. This indicates that the current maximum class scale corresponds to the 200-year maximum under the 4-degree global warming scenario, representing a significant finding warranting attention.

4.2 Changes in Annual Maximum Peak Discharge for 109 First-class River Basins Nationwide

The study area was expanded to include all 109 first-class river basins throughout Japan, enabling a quantitative analysis of changes in extreme flow events (Kobayashi *et al.*, 2020). For this analysis, the operation of major dams was incorporated into the 1K-DHM for all river basins. This rainfall-runoff model reflects anthropogenic flow control within the flow model to reproduce past floods. The bias in the annual maximum rainfall obtained from the d4PDF was corrected using analyzed rainfall data provided by the Japan Meteorological Agency. This corrected rainfall data was then used to estimate future changes in extreme flow.

4.2.1 Method of Analysis
The rainfall-runoff model 1K-DHM was applied to all first-class rivers nationwide. Flood control operations for major dams, whose catchment areas constitute 5% or more of the total basin area, were incorporated into the 1K-DHM. Model parameter values were identified for each river basin using observed flow data from past maximum floods since 2000. As a result, parameter values were obtained for the Nash coefficient (Nash and Sutcliffe, 1970) of 0.7 or greater and peak flow error rate of 20% or less for all water systems, including the effect of flood control by dam reservoirs. The Nash coefficient is a commonly used indicator of the reproducibility of observed discharge by rainfall-runoff models and is calculated using the following equation.

$$N_s = 1 - \frac{\sum_{i=1}^{I}(Q_i^{obs} - Q_i^{\square})^2}{\sum_{i=1}^{I}(Q_i^{obs} - \overline{Q^{obs}})^2} \quad \overline{Q^{obs}} = \frac{1}{I}\sum_{i=1}^{I} Q_i^{obs} \qquad (5)$$

In the above equation, Q_i represents the calculated flow rate at time step i, and Q_i^{obs} represents the observed flow rate at that time. I represents the number of hours of the subject flood event. A value of 1.0 indicates perfect agreement between the model-calculated and observed flow rates at the evaluation site, with values closer to 1.0 indicating higher reproduction accuracy. Generally, a value of 0.7 or higher indicates high simulation model reproducibility. The model was validated for floods of similar magnitude, and the results showed that approximately 80% of river basins had a Nash index of 0.7 or higher, and approximately 70% had a peak error rate of 25% or lower.

4.2.2 Results of Future Changes in the Frequency Distribution of Annual Maximum Discharge for 109 First-Class River Basins Nationwide
For the annual maximum discharge data obtained through rainfall-runoff simulations for each basin using 3,000 years of historical experiments and 5,400 years of 4-degree increase experiments, the Weibull formula was used to determine the flow rate corresponding to the design return period determined in the river improvement basic policy of each basin, which is referred to as the design calculation discharge hereafter. Figure 10 shows a scatter plot of the design flood discharge for the 109 first-class rivers and the design discharge obtained using the d4PDF past experiments. While the two do not strictly match due to differences in calculation methods and the rainfall data used, a good correspondence was observed. This is considered to demonstrate the rationality of rainfall-runoff calculations obtained using the d4PDF historical experiment data.

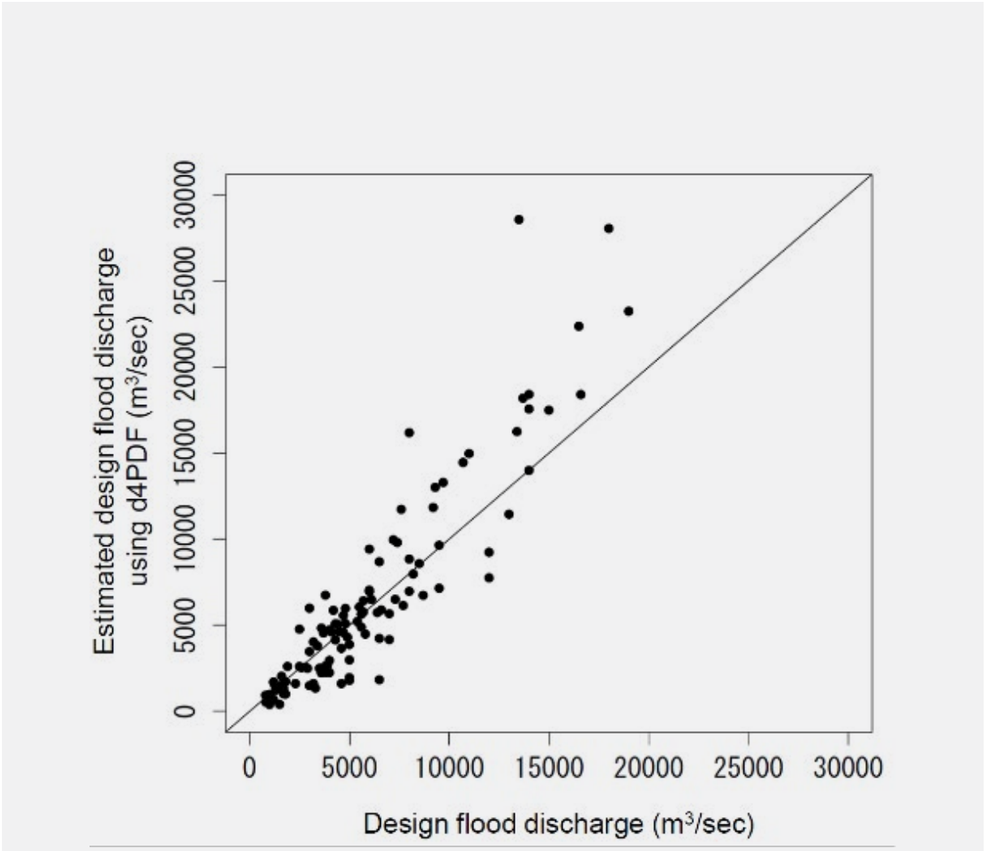

Figure 10: *Comparison of the design flood discharge for the 109 first-class rivers and the design discharge obtained using the d4PDF past experiments (from Kobayashi et al., 2020).*

We calculated the 100-year annual maximum flow rate for each basin, which is commonly used as a design flood for many first-class basins. We then obtained the increase rate in the 4-degree increase experiments relative to the past experiment for each basin to find regional differences as shown in Figure 11. The 4-degree increase experiments include six types of sea surface temperature ensemble prediction data (hereafter, SST ensembles).

The average increase rate of the 100-year probability flow rate across SST ensembles ranged from 1.11 for the smallest basin to 2.32 for the largest. In all basins the increase rate exceeded 1.0, indicating increased flow of the design return period for all basins. The increase rate was particularly high in the Hokkaido and Tohoku regions. The variation in increase rates between SST ensembles corresponded to the mean values of the increase rates, with larger variations observed in basins located further north.

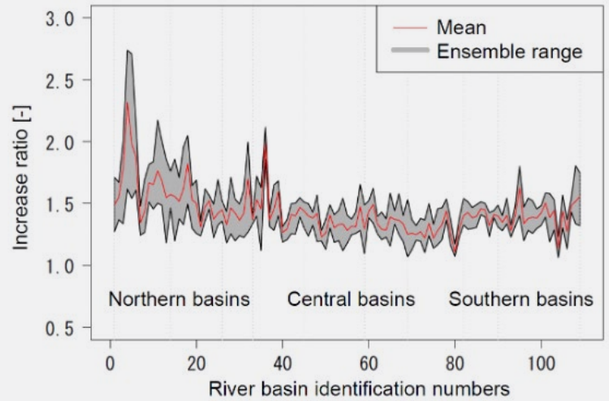

Figure 11: *Percentage increase in flood discharge of d4PDF historical experiment relative to 4-degree rise experiment for 100-year return period. The red line represents the average increase rate between the historical experiment and the 4-degree increase experiment, with the variation due to differences in SST patterns shown in gray color (from Kobayashi et al., 2020).*

Figure 12 shows maps of the return periods of the design flood for the first-class river basins designated in the basic river improvement policies for each river basin and the return periods of the design flood discharge of the d4PDF past experiment under the 4-degree increase experiment. While the return periods for the current design level range from 100 to 200 years, the 4-degree increase experiment results indicate that floods of the same magnitude occur in all watersheds with return periods of less than 60 years.

The differences in return periods in the 4-degree increase experiment generally corresponded to the return periods of the current design level. For basins with a return period of two hundred years, the return period decreased to 30–60 years; for basins with a return period of 150-year years, it decreased to 30–45 years; and for basins with a 100-year return period, it decreased to 30 years or less. Some watersheds even had return periods of 15 years or less.

4.2.3 Summary and Discussion

Bias correction was applied to precipitation data from past experiments, and the 4-degree increase experiment for d4PDF. The corrected rainfall data was input into the 1K-DHM model to calculate peak discharge for 109 first-class river basins nationwide.

The design-scale flood flow calculated using the d4PDF past experiments matched with the design flood discharge designated in the basic river improvement policies of each river basin, confirming the validity of the 1K-DHM. Calculations using the 4-degree increase experiment results showed that the 100-year probability flow increased in all river basins, with particularly high increase rates observed in Hokkaido, Tohoku, Hokushinetsu, and southern Kyushu.

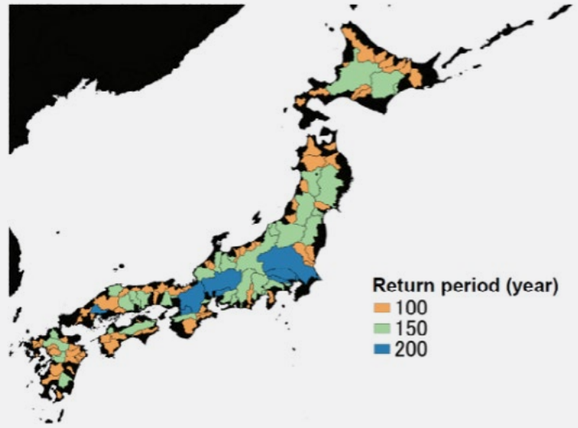

A) Return periods of design flood designated in the current flood control plans.

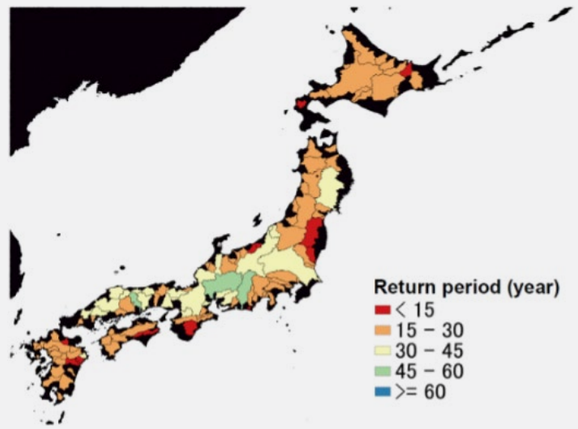

B) Return period of the design flood discharge at the current flood control planning level under the 4-degree increase experiment.

Figure 12: *Return period in flood control plans (top) and return period in the 4-degree increase experiment corresponding to the planned scale calculated flow rate from the d4PDF past experiment (bottom). (from Kobayashi et al., 2020).*

4.3 Future Changes in Extreme Flood Flows in Red River Basin Using d4PDF

Natural disasters occurring not only in Japan but also in other countries significantly impact Japan's economy. Particularly in Southeast Asia, many Japanese companies have established operations, and industrial parks in these countries have become production bases. To estimate flood risk in such regions, the distributed rainfall-runoff model 1K-DHM was applied to Red River basin that flows in China and Vietnam and flood flows in the basin was estimated using d4PDF precipitation data. Next, future changes in the annual maximum discharge at the Son-Tay station near Hanoi were predicted. Finally, the current and future occurrence frequency of river discharges equivalent to the 1971 flood scale was analyzed, which was considered the current development level, and the increase of the flood risk in this basin was classified (Kato *et al.*, 2020).

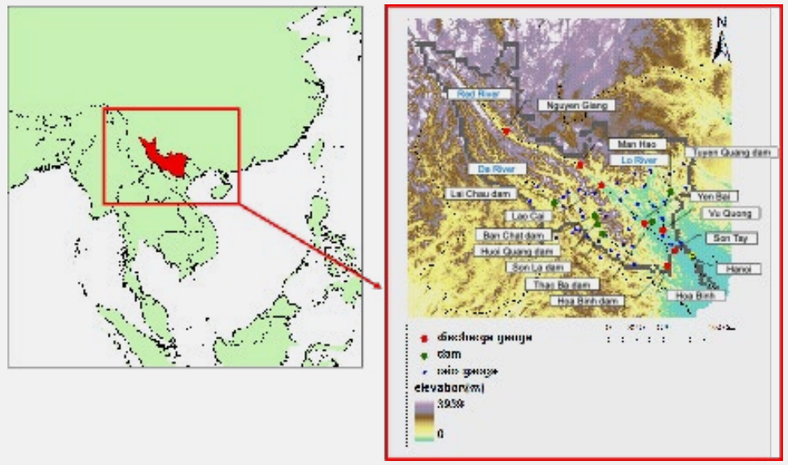

Figure 13: *Red River Basin (from Kato et al., 2020).*

4.3.1 Basin Overview

The Red River is an international river originating at the eastern edge of the Himalayas and flowing through China and Vietnam. Its drainage basin covers an area of 168,700 km2, approximately ten times larger than Japan's largest drainage basin, the Tone River. Upstream at the Son-Tay location, it joins the Da River and Lo River and flows through Hanoi City into the Gulf of Tonkin. Figure 13 shows a map of the Red River basin. The lower Red River Delta has a subtropical climate with an average annual precipitation of approximately 1,700mm. The rainy season runs from May to September, during which typhoon-induced flooding sometimes occurs.

The largest flooding on record occurred during a typhoon in 1971, with the maximum flow rate at the Son-Tay station reported as 37,400m^3/s. After this flood, flood control measures based on the Hanoi metropolitan area protection were implemented. The current discharge capacity at the Son-Tay station is estimated to be approximately 30,000m^3/s.

4.3.2 Analysis Method

A distributed rainfall-runoff model, 1K-DHM, with a 10 km resolution was constructed for the entire Red River basin. Parameter values of the 1K-DHM were identified using the SCE-UA method (Duan *et al.*, 1994), and then river discharge was predicted using the d4PDF precipitation data as input data. Observed precipitation data obtained from rain gauges were used for the Vietnamese territory and the APHRODITE Monsoon Asia precipitation dataset (APHRODITE-MA, http://aphrodite.st.hirosaki-u.ac.jp/products.html) was used for the Chinese territory.

For model parameter identification, hydrological data available at many observation sites were used. Model parameter values were identified for the 2002 flood, which was considered to be a valid data set from the water balance. The parameters d_c, d, n_s, k_a, β" and the equivalent roughness of the river channe n_r were identified as shown in Table 1 (left).

Generally, major rivers on continents have larger drainage areas than Japanese rivers, and river flow routing time spans several months. Therefore, evaporation must be considered when predicting river flow. Since observed evapotranspiration values are unavailable, an annual evaporation amount of 900 mm was set as a value with high reproducibility for river flow (Table-1 (right)). An annual evaporation amount of 900 mm is considered physically reasonable for the climate of this region. Then hourly evaporation was subtracted from precipitation and used as input data to runoff simulations. Since the rainfall-runoff mechanism adopted by the 1K-DHM is not suitable to apply to gently sloping basins with dry soils, the 1K-DHM was applied with the target period limited to the flood period. Figure 14 shows the river flow estimation results for the three sites: Hoa-Binh, Yen-Bai, and Vu-Quang. The temporal variation and peak flow of the river flow were generally reproduced.

Table 1: *Values of identified model parameter values (left) and evaluation of river flow simulations based on different annual evapotranspiration (right) (from Kato et al., 2020).*

Parameter	
Manning's roughness coefficient for the slope: n_s $(m^{-1/3}s)$	0.01
Hydraulic conductivity of the large void zone: *ka (m/s)*	0.01
Total porosity thickness in soil: *d (m)*	1.69
Porosity thickness in soil matrix: d_c *(m)*	1.00
Parameters related to hydraulic conductivity: *β (-)*	2.80
Manning's roughness coefficient for the channel: n_c $(m^{-1/3}s)$	0.03

Annual Evaporation (mm)	Nash coefficient
950	0.7542
900	0.7552
850	0.7547
800	0.7529
750	0.7497
700	0.7452

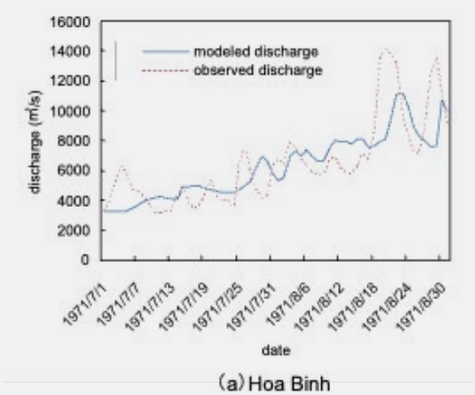

Figure 14: *River flow simulations at Hoa Binh (a), Yen Bai (b), and Vu Quang (c) (from Kato et al., 2020).*

4.3.3 Analysis results of future changes in the frequency distribution of annual maximum flow

River discharge was calculated using d4PDF precipitation data, and the frequency distribution of annual maximum discharge was obtained to estimate future changes. Since rainfall-runoff time lag to the Son-Tay site was estimated to be approximately 15 days, the frequency distributions of the annual maximum 15-day rainfall for the d4PDF past experiment and the 4-degree increase experiment were compiled. The results are shown in Figure 15.The frequency distribution from the d4PDF past experiment closely matched that from observed data (APHRODITE-MA). It was found that for the same occurrence frequency, the annual maximum 15-day precipitation increased in the 4-degree increase experiment.

d4PDF precipitation data for 6,000 years of past experiments and 5,400 years of 4-degree increase experiments were input into the 1K-DHM model to calculate runoff. Figure 16 shows the frequency distribution of annual maximum discharge at the Son-Tay site. The past experiment results were calculated without reflecting flow control by the dam. In the 4-degree increase experiment, discharge increases for all return periods.

The results indicate the 1971 flood, the largest flood on record, had a return period of approximately 6,000 years, confirming it was a largest class flood under the current climate condition. The return period for this flood in the 4-degree increase experiment, accounting for dam operation, decreased to approximately six hundred years, which raises concerns about increased frequency of large floods due to global warming. The return period corresponding to the current discharge capacity of 30,000 m^3/s near the Son-Tay site is approximately 300 years in the 4-degree increase experiment. While adequate flood control measures are currently in place, it was found that the risk of overtopping and breaching increases under global warming.

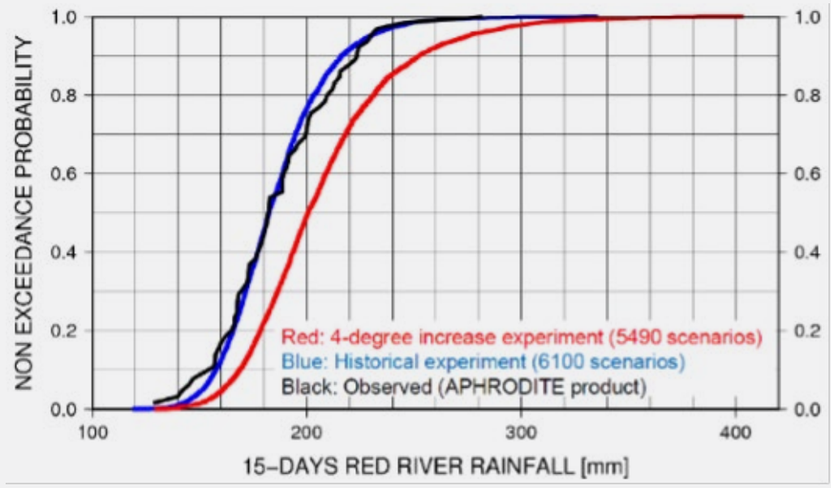

Figure 15: *Comparison of d4PDF and APHRODITE for the frequency distribution of the annual maximum 15-day average rainfall in the Red River basin (from Kato et al., 2020).*

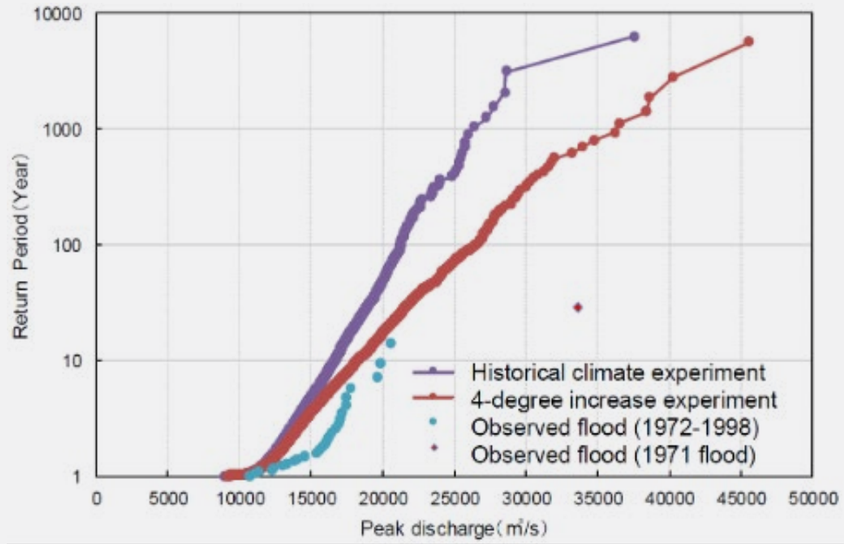

Figure 16: *Frequency distribution of annual maximum discharge at Son-Tay (from Kato et al., 2020).*

4.3.4 Summary and Discussion

Past experiments using d4PDF effectively reproduced the frequency distribution of the 15-day average basin precipitation corresponding to flood runoff duration. The 4-degree increase experiment showed an increase in annual maximum 15-day precipitation. Similarly, the 4-degree increase experiment indicated an increase in annual maximum river discharge.

The record-breaking 1971 flood, which is a largest-class flood under the current climate condition, would have a return period of approximately six hundred years under future climate conditions. The return period corresponding to the current discharge capacity of 30,000 m^3/s near the Son-Tay site could potentially decrease to approximately 300 years under the 4-degree increase scenario.

4.4 Future Changes in Extreme Flood Flow in Chao Phraya River Basin Using d4PDF

A rainfall-runoff model considering the characteristics of the Chao Phraya River basin in Thailand was constructed. Using bias-corrected d4PDF rainfall data as input, future changes in flood volume and peak discharge were forecasted. First, it was confirmed that the rainfall-runoff model could reproduce past floods and that the frequency distribution of annual maximum discharge at reference sites (Nakhon Sawan, C2 site) based on model calculations was consistent with observed discharge values. Next, future changes in the annual maximum discharge at C2 site were analyzed using the bias corrected rainfall. The cumulative flood volume exceeding 2,000 m^3/s at C2 site was also examined, which was an indicator for large-scale flood inundation around the Bangkok Metropolitan area. The results revealed that global warming increases flood risk in the Chao Phraya River basin (Kato *et al.*, 2022).

4.4.1 Basin Overview

The Chao Phraya River is Thailand's largest river, with a basin area of approximately 163,000 km^2, equivalent to about ten times the basin area of Japan's largest river, the Tone River. Four rivers originating in the northern mountainous region, the Ping, Wang, Yom, and Nan rivers, converge at the Nakhon Sawan site to form the Chao Phraya River, which flows through Ayutthaya and Bangkok into the Gulf of Thailand. Figure 17 shows a map of the Chao Phraya River basin. The average annual precipitation in the basin is approximately 1,200 mm, with evaporation at around 1,000 mm, meaning about 20% of rainfall becomes river runoff. The rainy season and dry season are clearly distinct, with the rainy season occurring from May to October.

4.4.2 Analysis Method

A 10 km resolution distributed rainfall-runoff model 1K-DHM was constructed for the Chao Phraya River basin. Parameters were identified using the SCE-UA method (Duan *et al.*, 1994), and river discharge was predicted using the d4PDF. To represent the reduction of the peak flow rate and delayed peak timing caused by flooding in the middle part of the Chao Phraya River basin, a linear reservoir model was introduced at the upstream of the Nakhon Sawan site, where flooding is prone to occur. Furthermore, the operation of two large dams at the upstream of the Chao Phraya River was modeled based on their rule curves and historical seasonal actual discharge records.

Input precipitation data primarily utilizes rain gauge observations, supplemented by the APHRODITE Monsoon Asia precipitation dataset. Evapotranspiration data was sourced from d4PDF. Hourly evapotranspiration data was multiplied by coefficients to conform to the annual water balance, then subtracted from precipitation data before input into the 1K-DHM. River flow simulations were conducted for rainy season considering the model characteristics of the 1K-DHM. Therefore, runoff calculations were performed after the annual cumulative precipitation reached 700 mm.

The identified model parameter values are shown in Table 2, and the results of reproducing the 2011 major flood inflow to the Bhumibol Dam using these parameters are shown in Figure 18.The Nash coefficient was 0.65, indicating that the time series of the hydrograph and the peak discharge were generally reproduced.

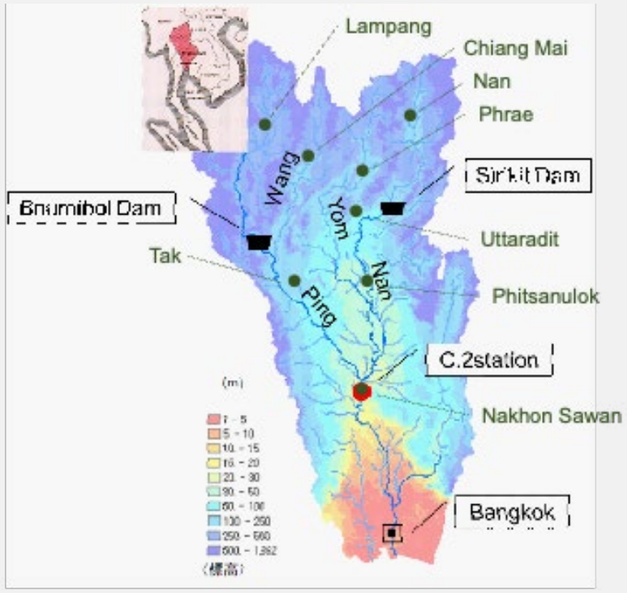

Figure 17: *Map of the Chao Phraya River Basin (from Kato et al., 2022).*

Table 2: *Values of identified model parameter (from Kato et al., 2022).*

Parameter		Value
Manning's roughness coefficient for the slope	n_s $(m^{-1/3}s)$	1.09×10^{-2}
Hydraulic conductivity of the large void zone	k_a (m/s)	7.17×10-3
Total porosity thickness in soil	d (m)	0.58
Porosity thickness in soil matrix	dc (m)	0.25
Parameters related to hydraulic coefficient	β $(-)$	8.28
Manning's roughness coefficient for the channel	n_c $(m^{-1/3}s)$	0.02

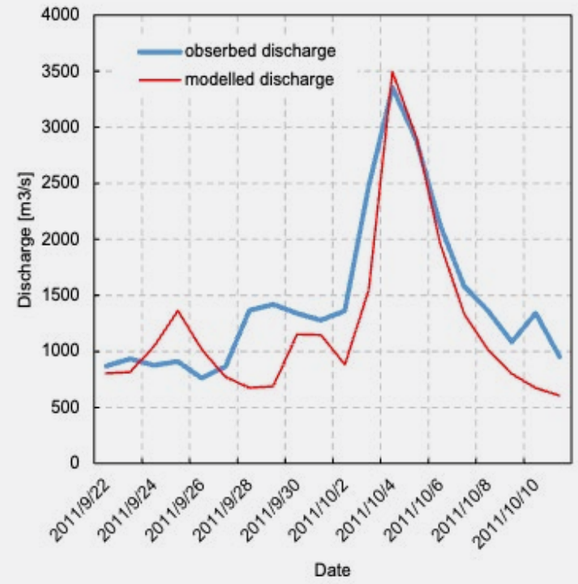

Figure 18: *Estimated in flow to the Bhumibol Dam (from Kato et al., 2022).*

4.4.3 Analysis results of future changes in annual maximum flow

Differences were observed between the statistical characteristics of d4PDF precipitation data and observed data. Therefore, the quantile mapping bias correction method was applied for each month to hourly precipitation values. The bias corrected precipitation data consists of 6,000 years for the historical experiment, 3,240 years for the 2-degree increase experiment, and 5,400 years for the 4-degree increase experiment. Next, these values were input into the 1K-DHM model to conduct discharge calculations. Figure 19 shows the future changes in annual maximum discharge and the cumulative volume exceeding 2,000m^3/s at the C2 site. Comparing observed discharge with the calculated ones from the historical experiments, both the annual maximum discharge and the cumulative volume exceeding 2,000 m^3/s showed good agreement with observed flood data.

Both the 2-degree and the 4-degree increase experiments yielded results exceeding the historical experimental values for the same return period. Looking at the future changes in extreme river flow corresponding to a 100-year return period, the annual maximum flow increased by 1.20 to 1.35 times from the historical experiments to the 2-degree increase experiment, by 1.55 to 1.63 times from the historical experiments to the 4-degree increase experiment, and by 1.21 to 1.30 times from the 2-degree increase experiment to the 4-degree increase experiment. This indicates that flow increases significantly with rising temperatures.

The cumulative exceedance flood volume above 2,000m^3/s at the C2 site showed even greater changes. The increase rate from the historical to the 2-degree increase experiment is 1.44 times to 1.67 times, from the historical to the 4-degree increase experiment is 2.23 times to 2.27 times, and from the 2-degree increase to the 4-degree increase experiment is 1.36 times to 1.55 times. This indicates that global warming increases the frequency of potential overtopping and breaching at the C2 site of the Chao Phraya River.

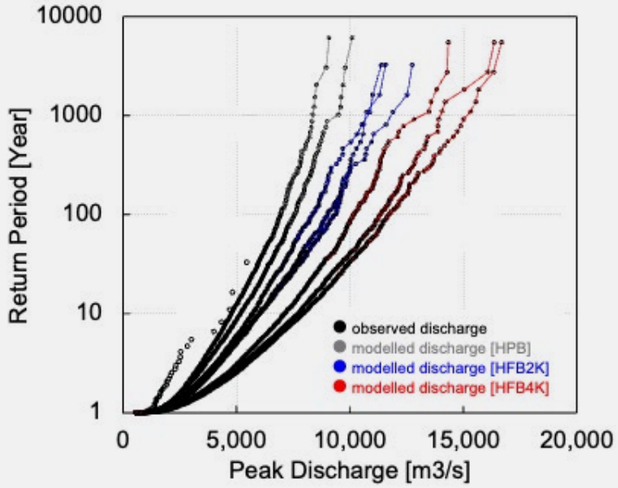

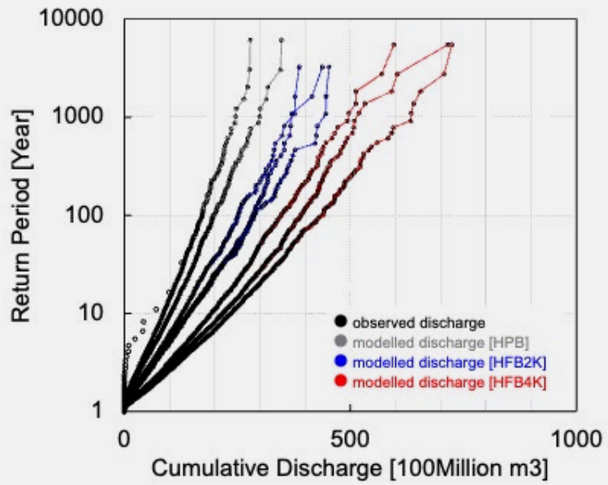

Figure 19: *Changes in the frequency distribution of annual maximum river discharge at the Nakhon Sawan (C2) site in the Chao Phraya River basin in Thailand. It shows differences between the historical experiment, 2-degree increase experiment, and 4-degree increase experiment (from Kato et al., 2022).*

4.4.4 Summary and Discussion

We applied the quantile mapping bias correction method to the d4PDF precipitation data and conducted river discharge calculations. In the Chao Phraya River basin, it was found that annual maximum discharge and cumulative discharge exceeding 2,000 m^3/s significantly increase with climate change. The change rates between the historical experiment (corresponding to a 100-year return period) and the 2-degree increase experiment are 1.20–1.35 times for the annual maximum discharge and 1.44–1.67 times for the cumulative discharge exceeding 2,000 m^3/s at the C2 site. The change rates between the past experiment and the 4-degree increase experiment were 1.55 to 1.63 times for the annual maximum flow and 2.23 to 2.27 times for the cumulative flow exceeding 2,000 m^3/s, indicating a significant increase in flood risk.

5.
Improving the Accuracy of River Flow Prediction Methods

Rainfall-runoff models have model parameters that determine the model's behavior. Quantitatively determining these values based on only information about topography, land cover, surface soil, and geology is difficult. In the analysis shown in the previous sections, the model parameters were identified to make the calculated predicted flow rate values close to the observed ones. Since hydrologic observation data is limited to specific locations, model parameters are usually optimized assuming the upstream areas have the same values as the observation site. The distributed rainfall-runoff model 1K-DHM described above can, in principle, determine model parameter values based on spatially distributed information about land cover, surface soil, and geology. Nevertheless, determining these values from soil samples collected in the field is not straightforward.

The values of soil parameter values obtained from the soil sample represent the soil at that specific location and cannot be used to parameter values representative of the entire soil type. This is likely due to the fact that even within the same topsoil, properties vary spatially, and the presence of large voids, which cannot be measured by soil samples, governs flow within the soil layers. Therefore, developing methods to derive average parameter values that represent the typical behavior of rainwater flowing within the soil layers across a given area based on spatially distributed land cover and soil information becomes a critical challenge. Achieving this would enable obtaining representative parameter values according to land cover and surface soil characteristics, thereby expanding the potential for predicting river discharge at arbitrary locations lacking hydrologic observation data. This section introduces research addressing these challenges.

5.1 Simultaneous Parameter Identification for a Distributed Rainfall-Runoff Model Incorporating Land Cover Information

In conventional model parameter identification, it is difficult to identify parameter values for each land cover type and surface soil type by considering their spatial distribution within the upstream catchment of a given flow observation site. Therefore, a possible method is to select observation points where the land cover in the upstream area is almost the same and identify the values of model parameters corresponding to the land cover contained there. However, such observation points are limited, which makes it difficult to identify parameter values for various land cover types. Therefore, we developed a method to identify model parameter values for multiple land covers and surface soils simultaneously for the distributed rainfall-runoff model 1K-DHM (Kato *et al.*, 2024).

5.1.1 Analysis Method

When using the SCE-UA method *(Duan et al., 1994)*, we devised an objective function to achieve optimal parameter identification calculations using multiple sites and multiple flood events, thereby developing a method to simultaneously identify model parameter values for different land cover types. The SCE-UA method was used for parameter identification calculations. The SCE-UA method is a type of global search method frequently used for parameter identification in rainfall-runoff models.

As an indicator of the performance of rainfall-runoff models to reproduce observed discharge, the Nash coefficient (Nash and Sutcliffe, 1970)

$$N_s = 1 - \frac{\sum_{i=1}^{I}(Q_i^{obs} - Q_i)^2}{\sum_{i=1}^{I}(Q_i^{obs} - \overline{Q^{obs}})^2} \quad , \overline{Q^{obs}} = \frac{1}{I}\sum_{i=1}^{I} Q_i^{obs} \qquad (5)$$

is often used to evaluate the reproducibility of observed discharge by rainfall-runoff models, which is also used as an objective function for parameter identification. In the above equation, Q_i and Q_i^{obs} represent the calculated discharge and observed discharge at time step i. I is the duration of the study flood event.

A value of 1.0 for this index indicates perfect agreement between the model calculation and the observed value, and values closer to 1.0 indicate higher reproduction accuracy. Generally, a value of 0.7 or higher is considered to indicate high reproducibility of the model calculation. Kato *et al.* (2024) extended the Nash coefficient in equation (5) and proposed six new indices to evaluate the reproducibility of calculated flow rates across multiple flood events and flow observation points. They identified parameters for each index and assessed their reproducibility. One of these indices is shown below.

$$Aall_1 = 1 - \frac{\sum_{k=1}^{K}\sum_{j=1}^{J_k}\sum_{i=1}^{I_{j,k}}\left(\frac{Q_{i,j,k}^{obs}}{A_j} - \frac{Q_{i,j,k}}{A_j}\right)^2}{\sum_{k=1}^{K}\sum_{j=1}^{J_k}\sum_{i=1}^{I_{j,k}}\left(\frac{Q_{i,j,k}^{obs}}{A_j} - \overline{q^{obs}}\right)^2} \quad \overline{q^{obs}} = \frac{\sum_{k=1}^{K}\sum_{j=1}^{J_k}\sum_{i=1}^{I_{j,k}} Q_{i,j,k}^{obs}}{J_k \times \sum_{k=1}^{K} I_{j,k}} \qquad (6)$$

Here, J is the number of observation points, K is the number of flood events, $I_{j,k}$ is the number of observation time steps for observation points j and flood events k,A_j is the grid number of the basin topography model upstream of observation points j (equivalent to the watershed area), $Q_{i,j,k}$ and $Q_{i,j,k}^{obs}$ are the calculated and observed discharge values for observation time i, observation point j and observation event k. This metric evaluates the difference between calculated and observed values for runoff height intensity, normalized by watershed area to account for differences in discharge magnitude between observation points.

5.1.2 Characteristics of the Identified Model Parameter Set

The distributed rainfall-runoff model 1K-DHM was applied to fifteen river basins in Kyushu. For the Kikuchi River basin (basin area 996 km^2), which includes multiple land cover types, the SCE-UA method was used to simultaneously estimate parameter values for each land cover type by maximizing the objective function in Equation (6).

The land cover categories to be identified are farmland, paddy field, mountainous areas, and urban areas. Their spatial distribution maps are shown in Figure 20 (top). The parameter values obtained for each land cover are shown in Table 3. The values of the top ten parameter sets obtained by the SCE-UA method showed that the parameter values for each land cover type were distributed within a narrow range, and clear differences appeared in the parameter values for each land cover type. Furthermore, since the relative magnitudes of these values reflect the physical characteristics of each land cover type, it is considered that parameter values reflecting the physical reality of the watershed could be identified.

5.1.3 Analysis Results and Discussion on Reproducibility

The reproducibility of flood simulations using the obtained parameter values was verified for five flood events across fifteen river basins (104 locations) in the Kyushu region, including the Kikuchi River basin. Figure 20 (top) shows the values of the evaluation index calculated using Equation (6). Locations with favorable evaluation indices are generally distributed without bias across each watershed. Furthermore, it is evident that locations with favorable Nash coefficients are distributed without bias between upstream and downstream areas in all watersheds.

Figure 20 (bottom) shows the distribution of the performance indices. Forty-one sites had evaluation indices between 0.5 and 0.8, while forty-seven sites had indices of 0.8 or higher. This confirmed that river flow can be reproduced with high accuracy, particularly in upper reaches with areas of 500 km^2 or larger. Identification calculations based on land cover data, covering multiple locations and multiple flood events, are an effective method. This confirmed the applicability of the simultaneous parameter identification for multiple land covers and surface soils simultaneously for the distributed rainfall-runoff model 1K-DHM.

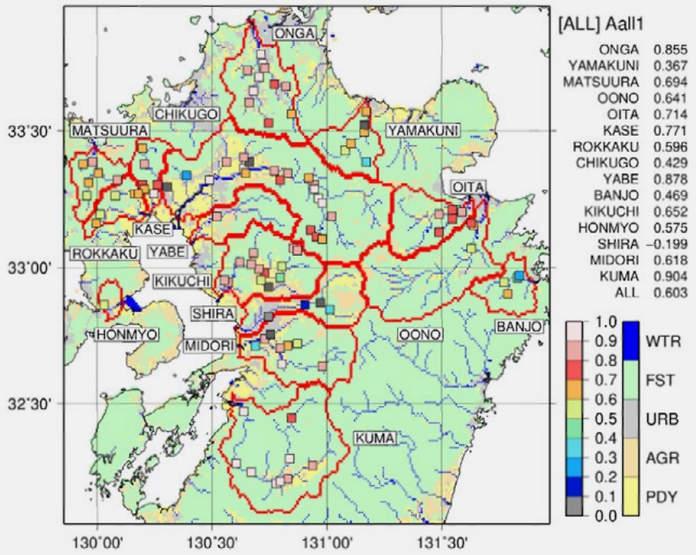

A) Land cover distribution map of northern Kyushu region and performance evaluation of flood forecasting using the equation (6).

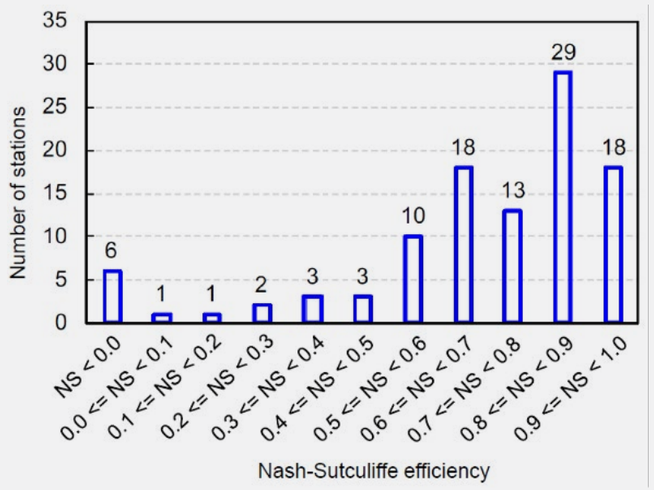

B) Frequency distribution of the performances of flood flow predictions.

Figure 20: *Land cover distribution map of the Kyushu region. WTR, FST, URB, AGR and PDY represent river channels, forests, urban areas, farmland, and paddy fields, respectively. The figure above shows the reproducibility evaluation values calculated using Equation (6) for each observation site. The lower figure shows the distribution of the number of observation points for flood prediction performance using Equation (6) (from Kato et al., 2024).*

Table 3: *Model parameter values identified by land cover types (from Kato et al., 2024).*

Parameter	Paddy field	Farmland	Forest	Urban
Manning's roughness coefficient for slopes: n_s $[m^{-1/3}s]$	1.47×10^{-1}	1.25	8.06×10^{-1}	6.78×10^{-1}
Hydraulic conductivity of the large void zone: k_a $[m/s]$	8.16×10^{-3}	5.02×10^{-2}	7.52×10^{-2}	5.79×10^{-3}
Porosity thickness of large void area: d_n $[m]$	0.00	0.00	1.10×10^{-1}	0.00
Porosity thickness in soil matrix portion: d_c: $[m]$	5.21×10^{-1}	8.91×10^{-1}	5.36×10^{-1}	0.00
Parameters related to hydraulic conductivity: β $[-]$	1.00×10	2.25	1.06×10	1.07×10
Manning's roughness coefficient for the channel: nc $[m^{-1/3}s]$	2.49×10^{-2}	3.58×10^{-2}	2.26×10^{-2}	2.89×10^{-2}

5.1.4 Summary and Discussion

We developed a method to simultaneously identify parameters for the distributed rainfall-runoff model 1K-DHM for each land cover type at multiple sites and using multiple flood events for the Kikuchi River. Next, we confirmed the reproducibility of discharge for multiple basins, sites, and flood events by applying the parameters obtained for the Kikuchi River to fifteen basins in northern Kyushu region.

The parameters identified based on the Kikuchi River's land cover showed good reproducibility at many sites. Among the 104 sites across all fifteen watersheds used for reproducibility verification, forty-one sites had a Nash coefficient of 0.5 or higher but less than 0.8, and forty-seven sites had a Nash coefficient of 0.8 or higher. This method is considered an effective approach for simultaneous parameter identification calculations using multiple sites and multiple flood events based on land cover types.

5.2 Simultaneous Parameter Identification for a Distributed Rainfall-Runoff Model Incorporating Surface Soil Information

The previous section presented a method for identifying parameter sets of a distributed rainfall-runoff model using land cover information. Since forest areas account for 67% of Japan's land area, the accuracy of flood prediction depends on whether appropriate parameter values can be set for forest areas. However, even within forest areas, the spatial distribution of surface soil and bedrock varies significantly. Numerous studies have shown that differences in surface soil and bedrock greatly influence rainfall-runoff phenomena. Therefore, the objective was to incorporate surface soil information in forest areas into the 1K-DHM to improve the reproducibility of rainfall-runoff phenomena (*Kato et al., 2025*).

5.2.1 Analysis Method

In addition to the land cover categories (farmland, paddy field, forest area, urban area) used in Figure 20 in the previous section, forest areas were further classified into andosols, brown forest soils, red-yellow soils, and other soils using soil map information from the National Agriculture and Food Research Organization (NARO). Figure 21 shows the land cover distribution map with added soil distribution. In the Kikuchi River basin, the area ratios of andosols, brown forest soils, and red-yellow soils within the forest area are 33.3%, 33.3%, and 26.9%, respectively, distributed almost evenly.

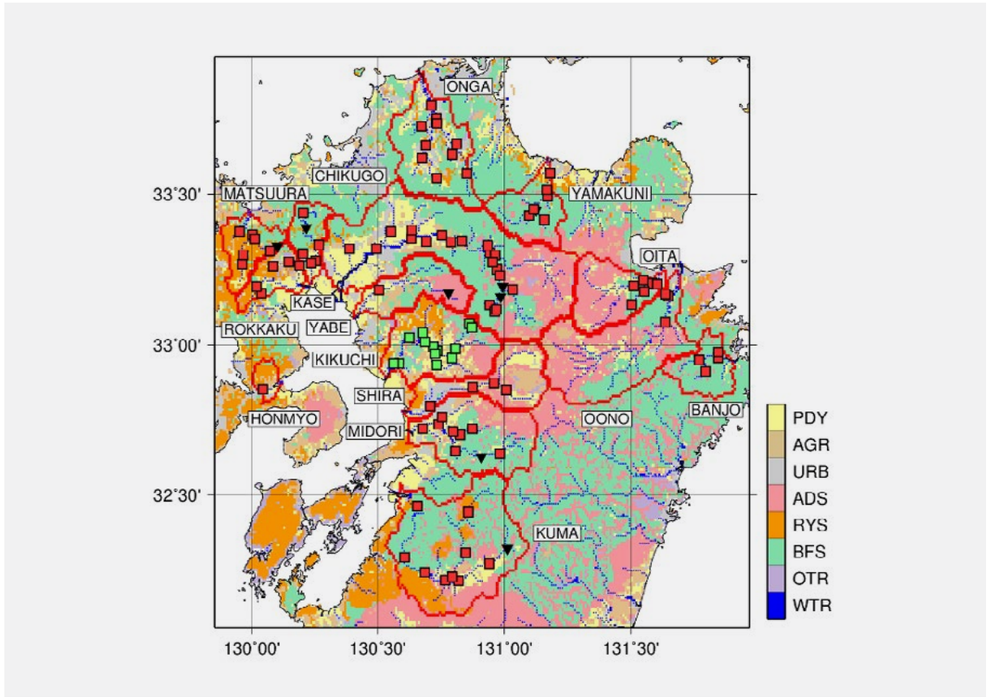

Figure 21: *Land cover with surface soil distribution map of northern Kyushu region. PDY, AGR, UBN, ADS, RYS, BFS, OTR, WTR represent paddy fields, farmlands, urban areas, andosols, red-yellow soils, brown forest soils, other soils, river, respectively. Squares represent observation points along the river channel. Observation points on the Kikuchi River used for parameter identification are shown in yellow green; observation points in the other fourteen basins are shown in red. ▼ indicates dam locations (from Kato et al., 2025).*

5.2.2 Characteristics of the identified model parameter set

Figure 22 shows the relationship between water depth h and unit width discharge q (h-q relationship) for slopes by using the optimally identified parameter values for each land cover type and surface soil type, which was generated by substituting the identified parameter values into equation (4) shown in Section 4.1(2). The slope gradient is was set to 0.1 for all cases. Figure 22 (top) shows the h-q relationships identified in the previous section for paddy fields, farmlands, forests, and urban areas. Figure 22 (bottom) shows the h-q relationships identified for forest areas classified into andosols, red-yellow soils, brown forest soils, and other soils.

Comparing these, the h-q relationship for the brown forest soil is similar to that of the forest, but the shapes of the ones for the andosols and the red-yellow soil are significantly different from the forest.

In particular, the andosol exhibited an h-q relationship with low discharge for the same water depth (soil moisture) and a slow runoff response, well representing the characteristics of the andosol. Conversely, the red-yellow soil yielded an h-q relationship showing a rapid runoff response. The h-q relationships of the urban area and farmland remained unchanged. The urban areas showed a rapid response and farmland showed an intermediate response. Only paddy fields changed to a rapid response function similar to urban areas. Since paddy fields are considered to have lower permeability and faster runoff response compared to forested areas, the newly identified h-q relationship for paddy fields is thought to be a valid relationship reflecting characteristics of other land cover types.

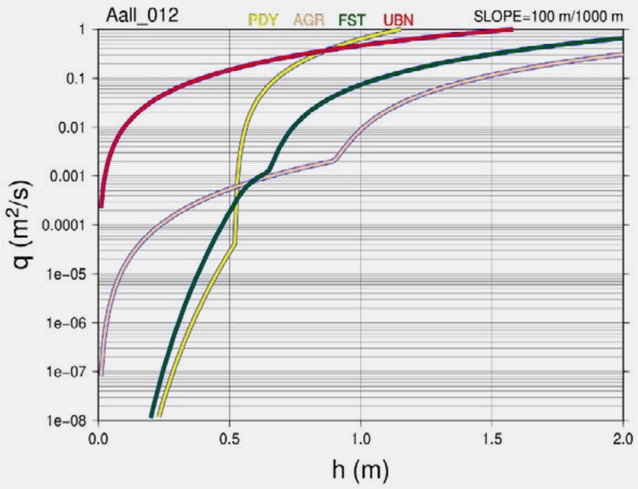

A h-q relationship equations obtained using only land cover information.

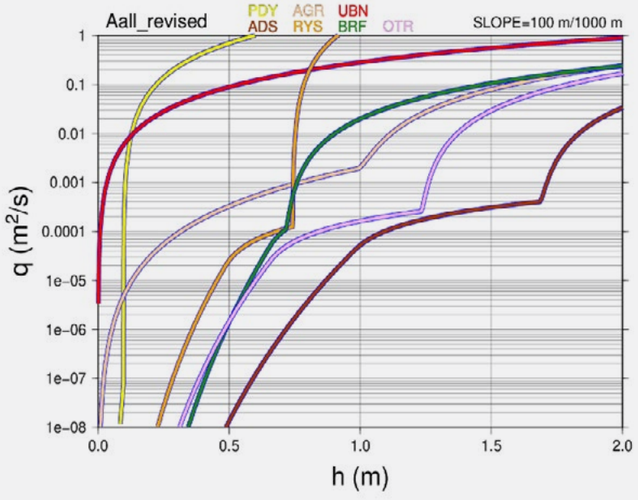

B h-q relationship equations obtained using land cover and surface soil information.

Figure 22: *h-q relationships by land cover and soil type. (a) shows the h-q relationships based on parameters identified reflecting only land cover distribution, while (b) shows the h-q relationships based on parameters identified reflecting both land cover and soil distribution. The horizontal axis represents water depth, and the vertical axis represents slope runoff per unit width. PDY, AGR, FST, UBN, ADS, RYS, BRF, OTR represents paddy field, farmland, forest, urban areas, andosols, red-yellow soil, brown forest soil, other soils, respectively (from Kato et al., 2025).*

5.2.3 Analysis Results and Discussion on Reproducibility

We examined how much the evaluation metrics improved by using both land cover and surface soil information for parameter identification compared to identification based only on land cover information. Eight categories are thought to be based on the improvement in the Nash coefficient after incorporating surface soil information, and the effect of incorporating soil distribution at each observation site were examined. Specifically, the eight categories shown in Table 4, G++, G+, G-, G--, B++, B+, B-, B are considered for each observation point. The spatial distribution of observation points classified into these eight categories is shown in Figure 23.

Table 4: *Setting out eight categories for the improvement of the Nash coefficient after reflecting surface soil information (from Kato et al., 2025)*

Improved Nash coefficient values after incorporating soil distribution information	Nash coefficient after soil reflection	
	0.5 or higher	Below 0.5
0.1 or higher	G++	B++
0 or more, less than 0.1	G+	B+
-0.1 or greater but less than 0	G-	B-
Below -0.1	G- -	B- -

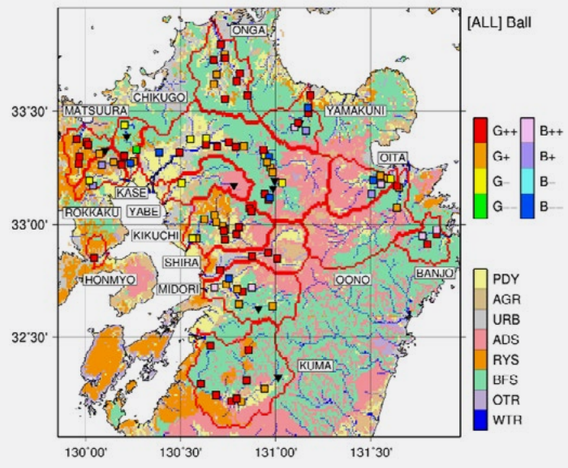

Figure 23: *Spatial distribution of surface soil information in the Kyushu region and the eight categories showing the improvement of Nash coefficients by reflecting the soil information. Squares along the river channel indicate observation points. Category classifications are shown for each point (from Kato et al., 2025)*

The observation points on the Kikuchi River used for parameter identification were classified as G++ or G+, with the exception of one point. Even for the points classified as G-, the deterioration in the Nash coefficient was extremely small. For the Kikuchi River, the Nash coefficient improved at nearly all points, yielding favorable values. For river basins other than the Kikuchi River, many observation points were classified as G++ or G+, while few were classified as B- or B-. On the other hand, the categories with the most significant deterioration in the Nash coefficient G- and B- were observed in several basins including the Oita River and the Kase River. It was also found that the categories B++, B+, B-, and B-, which still exhibited low Nash coefficient values even after accounting for soil distribution, were concentrated in certain basins.

5.2.4 Summary and Discussion

By incorporating surface soil distribution information, parameter values reflecting the runoff characteristics of andosols and red-yellow soils were obtained. Additionally, this also influenced the parameter values for paddy fields, yielding more realistic parameter values with quick runoff responses. As a result, the flow reproduction accuracy was improved for the observation points on the Kikuchi River where the parameter identification calculations were conducted. Furthermore, improved flow reproduction was also observed for observation points in the river basins which have similar land cover and soil characteristics with Kikuchi River basin. This result indicates the potential to obtain parameter values with even better reproduction accuracy by using multiple observation points with diverse characteristics.

6.
Future Challenges

As climate change progresses, increasing short-term precipitation intensity, it is necessary to predict changes in flood risk, make flood risk information accessible to all, and minimize flood damage.

Currently, the Japanese government is rapidly revising the "Basic Policy for River Improvement" for the 109 first-class river systems, incorporating climate change impacts. Moving forward, it is necessary to create flood hazard maps and flood risk maps under climate change scenarios and compare them with current ones to identify areas where flood hazards and risks may increase.

This information is indispensable for the national government's watershed flood control initiatives and also contributes to risk assessments for the private sector when building current industrial infrastructure or new infrastructure.

To enhance the accuracy of this risk information, improving precipitation information that causes flooding is essential. The d4PDF database introduced in this report is a groundbreaking resource with a large number of ensemble datasets required for flood risk assessment. While this report presented analysis results using d4DF data downscaled to a spatial resolution of approximately 20 km, higher-resolution precipitation data is needed to cover river basins in Japan, including small and medium-sized river basins. Fortunately, d4PDF data downscaled to a spatial resolution of 5 km has been created and is beginning to be utilized. By employing such high-resolution climate datasets, the development of flood risk information can advance even for small and medium-sized river basins, eliminating gaps in flood risk information coverage.

To enhance the accuracy of flood risk information, it is essential to improve the hydrological simulation models enabling flood and inundation prediction for any river basin, alongside the development of precipitation datasets as input information. As introduced in this report, the fundamental approach to predicting flood risk lies in improving the accuracy of river flow predictions. High-resolution spatial information on topography, land cover, surface soil, and geology is becoming increasingly available. There is an urgent need for regional generalization of rainfall-runoff simulation models using this information

A critical research challenge is to develop a rainfall-runoff simulation model applicable to all river basins that can predict river flow at any location, and to predict river flow with a certain degree of accuracy even in river basins where no hydrological observation information exists. The research introduced in Section 5 must continue to be advanced.

The development of such risk information should not be limited to river basins in Japan. Major flooding anywhere in the world can significantly impact the socio-economy of that region, which in turn would have an impact on the socio-economy of Japan. In order to contribute to the prevention and mitigation of water-related disasters around the world, and to ensure that Japanese companies and Japanese citizens with global operations are not affected by floods, it is necessary to develop flood forecasting methods that can be applied to any river basin in the world and generate water hazard and risk information. The joint research being conducted with Tokio Marine Research Institute, Inc. is based on an awareness of these issues and is indispensable research and development for building a sustainable society.

Acknowledgments

The river flow projections under the climate change scenarios presented in this report were obtained using the “Database for Policy Decision-Making for Future Climate Change” (d4PDF). The studies cited in Sections 4.3 and 4.4 of this report, concerning changes in the frequency and intensity of flood hazards due to climate change for rivers in Vietnam and Thailand, and the studies cited in Sections 5.1 and 5.2 concerning regional integration of a distributed rainfall-runoff model, were conducted as a joint research with Tokio Marine Research Institute, Inc. This report was prepared with the cooperation of Tokio Marine Holdings, Inc.

References

APHRODITE's Water Resources: Asian precipitation -highly-resolved observational data integration towards evaluation of extreme events, http://aphrodite.st.hirosaki-u.ac.jp/index.html

Duan, Q., Sorooshian, S., Gupta, V. K.: Optimal use of the SCE-UA global optimization method for calibrating watershed models, Journal of Hydrology , 158(3-4), pp. 265-284, 1994. https://doi.org/10.1016/0022-1694(94)90057-4

Ikebuchi, S., Shiiba, M., Takara, K., Tachikawa, Y.: Ace Hydrology, Asakura Publishing Co., Ltd., 1st Edition 1st Printing, 2006. 14th Printing, 2022. ISBN: 978-4-254-26478-4 C3351 https://www.asakura.co.jp/detail.php?book_code=26478&srsltid=AfmBOoqtb11K2t-QJMn0Au081OqGtTFP-Xxkm3hR0cReyee4FRdfmq0B

Japan Meteorological Agency, Atmosphere and Ocean Department, Meteorological Risk Management Division: Index representing rainfall disaster risk and hazard distribution of warnings, Weather Service Bulletin, 9(8), 2023. https://www.jma.go.jp/jma/kishou/books/sokkou/90/vol90_8.pdf

Japan Meteorological Agency: Climate Change in Japan 2025 – Report on assessment of observed/projected climate change relating to the atmosphere, land, and ocean, https://www.data.jma.go.jp/cpdinfo/ccj/index.html

Kanamaru, S. and Takasao, T.: Hydrology, Civil Engineering Lecture Series 4, Asakura Publishing Co., Ltd., 1975.

Kato, D., Kato, M., Tanaka, T., Feng, S., Tachikawa, Y.: Parameter regionalization based on land-use types for a distributed rainfall-runoff mode, Journal of Japan Society of Civil Engineers, 80(12), 24-00068, 2024, https://doi.org/10.2208/jscejj.24-00068

Kato, D., Kato, M., Tanaka, T., Feng, S., Tachikawa, Y.: Parameter regionalization based on land-use types and soil types for a distributed rainfall-runoff model, Journal of Japan Society of Civil Engineers, 81(11), 25-00052. 2025, https://doi.org/10.2208/jscejj.25-00052

Kato, D., Shinohara, M., Nagano, T., Kato, M., Tsuboki, K., Tanaka, T., Tachikawa, Y., Nakakita, E.: Estimating future changes of extreme river discharge in the Red River, Vietnam using d4PDF, Journal of Japan Society of Civil Engineers, B1(Hydraulic Engineering), 76(1), pp. 107-117, 2020, https://doi.org/10.2208/jscejhe.76.1_107

Kato, D., Shinohara, M., Kato, M., Tsuboki, K., Tanaka, T., Tachikawa, Y.: Estimating future changes of extreme river discharge in the Chao Phraya River using d4PDF with multiple bias corrections, Journal of Japan Society of Civil Engineers, B1(Hydraulic Engineering), 78(1), pp. 35-47, 2022, https://doi.org/10.2208/jscejhe.78.1_35

Kobayashi, K., Tanaka, T., Shinohara, M., Tachikawa, Y.: Analyzing future changes of extreme river discharge in Japan using d4PDF, Journal of Japan Society of Civil Engineers, B1 (Hydraulic Engineering), 76(1), pp. 140-152, 2020, https://doi.org/10.2208/jscejhe.76.1_140

Kyoto University Graduate School of Engineering, Department of Civil and Earth Resources Engineering, Hydrology and Water Resources Research Laboratory: 1K-FRM/DHM, A distributed flood routing model and distributed hydrologic model based on kinematic wave theory using HydroSHED topography data, 2020, https://hywr.kuciv.kyoto-u.ac.jp/products/1K-DHM/1K-DHM.html

Ministry of Land, Infrastructure, Transport and Tourism, Water Management and Land Conservation Bureau: Technical Standards for River and Stream Erosion Control - Planning Manual (Basic Planning Manual), as of August 2025. https://www.mlit.go.jp/river/shishin_guideline/gijutsu/gijutsukijunn/keikaku/index.html

Ministry of Land, Infrastructure, Transport and Tourism: Technical study committee on flood control planning considering climate change: Proposal on "Approaches to Flood Control Planning Considering Climate Change," Revised April 2021, https://www.mlit.go.jp/river/shinngikai_blog/chisui_kentoukai/

Mizuta R., Murata A., Ishii M., Shiogama H., Hibino K., Mori N., Arakawa O., Imada Y., Yoshida K., Aoyagi T., Kawase H., Mori M., Okada Y., Shimura T., Nagatomo T., Ikeda M., Endo H., Nosaka M., Arai M., Takahashi C., Tanaka K., Takemi T., Tachikawa Y., Temur K., Kamae Y., Watanabe M., Sasaki H., Kitoh A., Takayabu I., Nakakita E., Kimoto M.: Over 5,000 years of ensemble future climate simulations by 60-km global and 20-km regional atmospheric models, Bulletin of the American Meteorological Society, 98(7), pp. 1383-1398, 2017. https://doi.org/10.1175/BAMS-D-16-0099.1

Nash, J. E. and Sutcliffe, J. V: River flow forecasting through conceptual models part I -A discussion of principles, Journal of Hydrology, 10(3), pp. 282–290, 1970. https://doi.org/10.1016/0022-1694(70)90255-6

National Agriculture and Food Research Organization: Japanese Soil Inventory, 1:200,000 scale soil map, https://soil-inventory.rad.naro.go.jp/offer.html

Shiiba, M., Tachikawa, Y., Ichikawa, Y.: Hydrology and Hydraulic Engineering Planning, Chapter 1: Surface flow, Kyoto University Press, 2013. ISBN: 9784876982479, https://www.kyoto-up.or.jp/book.php?id=1865

Tachikawa, Y. Miyawaki, K., Tanaka, T, Yorozu, K. Kato, M., Ichikawa, Y., Kim, S.: Future change analysis of extreme floods using large ensemble climate simulation data, Journal of Japan Society of Civil Engineers, B1 (Hydraulic Engineering), 73(3), pp. 77-90, 2017, https://doi.org/10.2208/jscejhe.73.77

Issuer
Professor **TACHIKAWA Yasuto**
Department of Civil and Earth Resources Engineering
Graduate School of Engineering
Kyoto University

Sponsored by
Tokio Marine Holdings Inc.

Date of Issue
March 2026

TOKIO MARINE
GROUP